HHS Public Access

Author manuscript

Dev Cell. Author manuscript; available in PMC 2021 March 29.

Published in final edited form as:

Dev Cell. 2021 February 08; 56(3): 277–291.e6. doi:10.1016/j.devcel.2020.11.017.

Embryonic Stem Cell-Derived Extracellular Vesicles Maintain ESC Stemness by Activating FAK

Yun Ha Hur[1], **Shi Feng**[2], **Kristin F. Wilson**[1], **Richard A. Cerione**[1,2,3,*], **Marc A. Antonyak**[1]

[1]Department of Molecular Medicine, Cornell University, Ithaca, NY 14853, USA

[2]Department of Chemistry and Chemical Biology, Cornell University, Ithaca, NY 14853, USA

[3]Lead Contact

SUMMARY

It is critical that epiblast cells within blastocyst-stage embryos receive the necessary regulatory cues to remain pluripotent until the appropriate time when they are stimulated to undergo differentiation, ultimately to give rise to an entire organism. Here, we show that exposure of embryonic stem cells (ESCs), which are the *in vitro* equivalents of epiblasts, to ESC-derived extracellular vesicles (EVs) helps to maintain their stem cell properties even under culture conditions that would otherwise induce differentiation. EV-treated ESCs continued to express stemness genes, preserving their pluripotency and ability to generate chimeric mice. These effects were triggered by fibronectin bound to the surfaces of EVs, enabling them to interact with ESC-associated integrins and activate FAK more effectively than fibronectin alone. Overall, these findings highlight a potential regulatory mechanism whereby epiblast cells, via their shed EVs, create an environment within the blastocyst that prevents their premature differentiation and maintains their pluripotent state.

In Brief

Virtually all cells form and release multiple distinct classes of extracellular vesicles, including microvesicles and exosomes, to communicate with their surroundings. Here, Hur et al. show that embryonic stem cells use this form of intercellular communication as a mechanism to help maintain the pluripotency of the stem cell niche.

Graphical Abstract

*Correspondence: rac1@cornell.edu.

AUTHOR CONTRIBUTIONS

Y.H.H. designed and performed experiments and wrote the manuscript. S.F. generated the electron microscopy images. K.F.W., R.A.C., and M.A.A. designed experiments and wrote the manuscript.

SUPPLEMENTAL INFORMATION

Supplemental Information can be found online at https://doi.org/10.1016/j.devcel.2020.11.017.

DECLARATION OF INTERESTS

The authors declare no competing interests.

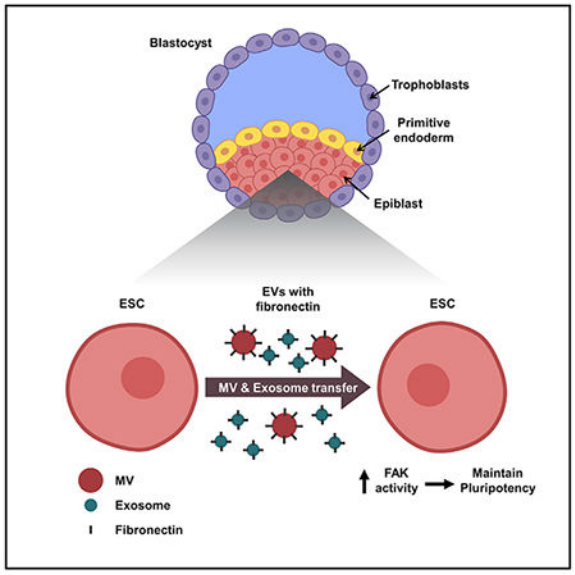

INTRODUCTION

Embryonic stem cells (ESCs) are highly specialized pluripotent cells that either undergo self-renewal or differentiate into virtually any cell type (Evans and Kaufman, 1981). Although ESCs can be maintained in their pluripotent state using defined culture conditions, in the physiological setting, their pluripotent counterparts are only transiently present during a specific stage of early development (Gardner and Cockroft, 1998; Snow, 1977). Specifically, these cells are contained within the epiblast layer of the inner cell mass (ICM) of blastocyst-stage embryos. The ICM also contains the primitive endoderm and is surrounded by a layer of trophoblasts referred to as the trophectoderm. At this stage of development, the cells that make up the epiblast are considered to be pluripotent due to the expression of several core stemness transcription factors, including Oct3/4 (Nichols et al., 1998) and Nanog (Mitsui et al., 2003). However, they rapidly lose their stem cell identity by downregulating the expression of the core stemness proteins (Thomson et al., 2011; Chambers et al., 2003; Kashyap et al., 2009). They then undergo epigenetic alterations that activate a distinct set of transcriptional machinery (Dodge et al., 2004; O'Carroll et al., 2001; Tachibana et al., 2002), which cause them to differentiate into the germline as well as the three primary germ layers, namely ectoderm, mesoderm, and endoderm, that will eventually give rise to every tissue and organ within an organism (Murry and Keller, 2008). While it is well established that cell fate decisions (i.e., determining whether to remain pluripotent or undergo differentiation) need to be tightly controlled for proper development (Young, 2011), an understanding of the mechanisms responsible for mediating these cellular transitions is still lacking. This is especially true with regard to how the pluripotency of the cells that comprise the epiblast is maintained in the early embryo.

Extracellular vesicles (EVs) have emerged as an important form of intercellular communication and are attracting significant attention due to their roles in several different physiological and pathological processes. One of the major classes of EVs is exosomes,

small intraluminal vesicles, ranging in size from 30 to 150 nm in diameter, which are formed within multivesicular bodies (MVBs) and trafficked to the cell surface. MVBs fuse with the plasma membrane and release their contents, i.e., exosomes, into the extracellular space. The other major class of EVs is most often referred to as microvesicles (MVs), although they are sometimes described in literature as shedding vesicles or large EVs. MVs range from 0.2 to 1.0 μm in diameter and are formed as a result of their outward budding and fission from the plasma membrane (Desrochers et al., 2016a; Latifkar et al., 2019).

A variety of proteins, RNA transcripts, and micro-RNAs have been shown to be associated with MVs and exosomes. This cargo is often localized within the lumen of EVs, although, in some cases, it is associated with the vesicle surface (Jeppesen et al., 2019; Valadi et al., 2007; Desrochers et al., 2016b; Ratajczak et al., 2006). Importantly, MVs and exosomes can engage and transfer their cargo to other (i.e., recipient) cells and in doing so, alter cellular behavior. The roles of EVs in cancer progression have been studied extensively, and they have been found to help shape the tumor microenvironment, promote immunosuppression, and enhance cancer cell growth, survival, invasion, and metastatic spread (Antonyak and Cerione, 2014; Antonyak et al., 2011; Costa-Silva et al., 2015; Kreger et al., 2016; Van Niel et al., 2018). However, EVs have, in fact, also been shown to impact a wide range of physiological processes. One interesting example is stem cell biology. We recently described how the larger-sized EVs (i.e., MVs) produced by pluripotent cells in the ICM can be transferred to the trophectoderm in blastocysts to promote implantation, an early step in pregnancy in which the developing embryo attaches and invades into the uterus (Desrochers et al., 2016b). In the studies presented below, we now describe how EVs provide a mechanism for intercellular communication that enables ESCs to maintain their stem cell lineage.

RESULTS

ESCs Generate and Release Large Quantities of EVs

An important question in developmental and stem cell biology concerns the underlying mechanism by which the pluripotency of the cells that comprise the epiblast is maintained. One intriguing idea is that EVs play an important role in this process by ensuring that these cells remain in a pluripotent state until the appropriate time when they undergo their specific cell fate transitions. In order to test this idea, we established ESC cultures, which are considered to be the *in vitro* counterparts of epiblast cells (Nichols et al., 2009) and examined their ability to generate the two classes of EVs. A feeder cell-independent mouse ESC line was maintained in a medium supplemented with GSK3β and MEK1/2 inhibitors (2 inhibitors; 2i), together with leukemia inhibitory factor (LIF), referred to as 2i+LIF medium (Ying et al., 2008). Under these conditions, ESCs expressed their full complement of core stemness proteins, including Oct3/4, Nanog, Sox2, c-Myc, and Klf4, as detected by western blot analysis and immunofluorescence microscopy (Figures 1A and S1A). In contrast, differentiated mouse embryonic fibroblasts (MEFs) showed little or no detectable expression of these proteins, with the exception of Klf4; whereas, as expected, they expressed the fibroblast marker, Thy1 (Rege and Hagood, 2006). Karyotyping chromosome spreads of

ESCs stained with DAPI confirmed that they contained the proper number of chromosomes and that there were no obvious chromosomal abnormalities (Figure S1B).

Two different assays were performed for assessing ESC pluripotency: sphere formation (Pastrana et al., 2011; Tamm et al., 2013) and alkaline phosphatase (AP) activity (Takahashi and Yamanaka, 2006; Takahashi et al., 2007; Thomson et al., 1998). Figures 1B and S1C show that ESCs formed spheres under these defined culture conditions, which were maintained for at least 5 additional passages (Figure S1D), and nearly all of the ESC spheroids were positive for AP activity (Figures 1C and S1E). As anticipated, MEFs failed to form spheres and lacked detectable AP activity (Figures 1B, 1C, S1C, and S1E).

To determine the relative amounts of MVs and exosomes generated by ESCs, the conditioned medium was collected from multiple cultures containing equivalent numbers of ESCs and subjected to consecutive low-speed centrifugations (i.e., 1,0 × *g*, 5 min) to remove cells and large debris. The media were then analyzed by nanoparticle tracking analysis (NTA) to determine the size and number of EVs present in the samples. ESCs produced ~3.5-fold more exosomes (~50–150 nm in diameter) than MVs (200 and 450 nm in diameter) (Figure 1D). Negative-stain electron microscopy images of these two sets of ESC-derived EVs are shown in Figure S1F.

The two classes of EVs shed by ESCs were resolved through a series of steps that included low-speed centrifugation, filtration using a 0.22 μm filter, and ultracentrifugation (Figure S1G). The EV preparations, as well as the ESCs (whole cell lysates; WCL), were lysed and examined for EV markers by western blot analysis. The general EV marker, Flotillin-2 (Desrochers et al., 2016b; Li et al., 2012), was present in both the MV and exosome preparations (see lanes labeled MVs and Exo), while the exosome-specific marker, CD9 (Andreu and Yáñez-Mó, 2014; Willms et al., 2018), was detected only in the exosome fraction (Figure 1E). The cytosolic signaling protein, focal adhesion kinase (FAK), was not detected in either the MV or exosome preparations, confirming that they were devoid of cytosolic contaminants. The ESC-derived MVs and exosomes were further resolved by sucrose density gradient sedimentation. Twelve distinct fractions from each EV preparation were collected and pooled together in groups of four, representing low-, intermediate-, and high-density fractions. MVs were enriched in the intermediate-density fractions, as detected using a Flotillin-2 antibody, whereas CD9-positive exosomes were predominantly present in the intermediate- and high-density fractions (Figure 1F), consistent with previous findings (Jeppesen et al., 2019).

We then determined whether the EVs shed by ESCs were capable of binding to other ESCs. The conditioned medium collected from ESCs was incubated with the fluorescent membrane dye, FM1-43FX, and then the EVs were isolated from the medium as described in Figure S1G. This approach labels the EVs and removes any soluble (unincorporated) dye. ESCs were treated with the isolated MVs and exosomes for 1 h, at which point the cells were washed thoroughly to remove any free EVs, fixed, and visualized using brightfield and fluorescent microscopy. As shown in Figure 1G, the majority of ESCs treated with FM1-43FX-labeled MVs or exosomes exhibited fluorescence, indicating that the ESC-derived EVs associated with the ESCs.

EVs from ESCs Promote Stem-Cell-Related Phenotypes

The decision of whether the cells within the epiblast layer of blastocyst-stage embryos remain in their pluripotent state or undergo the transition to a specific cellular lineage is a highly regulated process (Nishikawa et al., 2007). Therefore, we set out to determine whether the EVs shed by ESCs could potentially play an important role in this regulation. First, we established culturing conditions that caused ESCs to lose their pluripotency and undergo differentiation. This was achieved by changing the medium used to maintain ESCs in their pluripotent state (i.e., the 2i+LIF medium) to a medium that lacked GSK3β and MEK1/2 inhibitors as well as LIF (referred to as N2B27 medium). When ESCs were cultured in this medium for 3 days, their growth rate was markedly slowed (Figure 2A), with ~70% of the ESCs undergoing cell death when grown in N2B27 medium for 5 days (Figure 2B). However, the remaining viable cells began to undergo differentiation. They attached to the plate as single cells, often exhibited protrusions (Figure S2A, arrows), and no longer expressed the pluripotent proteins Oct3/4 and Nanog (Figures 2C and S3, compare the top and middle panels). These cells also exhibited the epigenetic changes characteristic of cells undergoing differentiation (Surani et al., 2007; Boland et al., 2014), such as increases in the trimethylation of lysine 27 in histone H3 (H3K27me3) (Juan et al., 2016; Petruk et al., 2017) (Figure 2C). Moreover, they were incapable of forming spheroids and lacked AP activity (Figures 2D, 2E, S2B, and S2C).

We next examined how ESC-derived MVs and exosomes affected ESCs that were being cultured under differentiation conditions. Whereas the growth of ESCs cultured in N2B27 medium had slowed considerably; when the cells were treated with equivalent numbers of MVs, exosomes, or a combination of both, their rate of growth increased nearly 2-fold compared to untreated control cells (Figure 3A). The same treatments with EVs also inhibited cell death caused by culturing ESCs in N2B27 medium for 5 days, reducing the amount of dying cells from ~70% to less than 30% (Figure 3B).

ESCs grown in N2B27 medium for 5 days exhibited a markedly reduced expression of Oct3/4 and Nanog (Figure 3C, compare lanes 1 and 2), which was accompanied by an increase in the expression of the differentiation marker, H3K27me3. However, when these cells were treated with MVs and/or exosomes isolated from pluripotent ESCs, their ability to express the core stemness proteins Oct3/4 and Nanog was restored, while H3K27me3 expression was essentially eliminated (Figures 3C, compare lanes 2 to lanes 3–5, and S3). ESCs that were cultured under differentiation conditions and treated with either MVs or exosomes from pluripotent ESCs also retained their ability to form spheres and express AP activity (Figures 3D–3F). The combination of MVs and exosomes typically gave rise to an enhanced effect, generating larger and greater numbers of spheres, compared to when cells were treated with either MVs or exosomes alone (Figures 3D and 3E).

Similar results were obtained when MVs and exosomes derived from ESCs were used in blastocyst outgrowth assays. Blastocyst-stage embryos were isolated from pregnant mice and cultured in a dish. Typically, within 4–5 days, the trophoblasts that surrounded the ICM attached to the dish and migrated (i.e., they exhibited outgrowth), while the cells that comprised the epiblast layer of the ICM lost their pluripotency and differentiated, as indicated by a reduction in the expression of the pluripotent markers Oct3/4 and Nanog

(Figure 3G, top panel). However, when outgrowth assays were carried out on blastocysts treated with MVs and exosomes from ESCs, several of the cells in the epiblast continued to express these proteins (Figures 3G, bottom panel, and 3H).

Importantly, we wanted to see whether these observations would extend into *in vivo* models. Therefore, we next examined whether treating ESCs cultured under differentiation conditions with ESC-derived EVs retained their ability to generate a chimeric animal (Beddington and Robertson, 1989; Hu et al., 2013; DeChiara et al., 2010). ESCs grown in either 2i+LIF medium or N2B27 medium, with or without supplementation with MVs and exosomes from pluripotent ESCs, were lysed and analyzed by western blotting using a Nanog antibody. Consistent with previous findings (Abranches et al., 2009; Thomson et al., 2011), ESCs cultured in N2B27 medium for only 1–2 days started to undergo differentiation and began to lose the expression of pluripotent markers such as Nanog (Figure 4A, compare lanes 1 and 2). However, treatment of these cells with ESC-derived EVs prevented this outcome (Figure 4A, compare lanes 2 and 3). The EV-treated cells cultured in N2B27 medium were collected and injected into embryonic-day 3.5 (E3.5) blastocysts. The blastocysts were then surgically placed into the uteri of surrogate mice (Figure 4B). The ability of ESCs to successfully incorporate into the embryos and give rise to a chimeric mouse was confirmed by changes in the coat color of the offspring. Specifically, the incorporation of ESCs would result in pups that have white and black-colored coats, while a lack of ESC integration would yield pups with white coat color. EV-treated ESCs cultured in N2B27 medium were able to give rise to chimeric mice (Figure 4C) and exhibited an efficiency of integration, similar to that for cells maintained in 2i+LIF medium (Figure 4D).

EVs Promote Stemness by Increasing FAK Activation in Recipient Cells

We initially considered the possibility that ESC-derived EVs helped maintain a stem cell phenotype by mediating the transfer of core stemness proteins and/or their RNA transcripts to recipient cells, as has been previously suggested (Ratajczak et al., 2006; Katsman et al., 2012). Western blot analysis performed on the MV and exosome fractions collected from ESCs showed that they contained extremely low, and in most cases, undetectable levels of the core stemness proteins Oct3/4, Nanog, Sox2, Klf4, and c-Myc (Figure S4A). The amounts of RNA transcripts associated with the ESC-derived MVs were also very low (Figures S4B and S4C). However, the exosomal fractions collected from ESCs contained a significant amount of RNA (Figure S4B). Reverse transcriptase (RT)-PCR performed on the exosomal RNA, using primer sets that amplify Oct3/4 and Nanog, showed that these transcripts were associated with the exosomes (Figure S4C). Likewise, the transcripts encoding several additional pluripotent proteins (i.e., Klf4, c-Myc, and Lin28) could be PCR-amplified from the same RNA sample, with the exception of Sox2 (Figure S4D, lane 2). Treating intact exosomes that were freshly isolated from ESCs with RNase A resulted in the complete degradation of the RNA transcripts encoding pluripotent proteins (Figure S4D, compare lanes 2 and 3), indicating that the transcripts are associated with the outer surfaces of the exosomes, consistent with what was reported for the association of RNA with exosomes shed by cancer cells (Jeppesen et al., 2019). We then found that exosomes treated with RNase A were as efficient as untreated (control) exosomes at maintaining the expression of Oct3/4 and Nanog in ESCs cultured under differentiation conditions (Figure

S4E). Therefore, neither the transfer of core stemness proteins nor the RNA transcripts encoding these proteins can account for the ability of ESC-derived EVs to promote stem cell-like characteristics.

Next, we examined whether EVs produced by pluripotent ESCs were able to activate signaling proteins in ESCs cultured in N2B27 medium, i.e., similar to EVs derived from aggressive cancer cells that stimulate signaling activities in recipient cells and give rise to marked phenotypic changes (Antonyak et al., 2011; Li et al., 2012). We found that the most striking change occurred with FAK. Specifically, treatment of ESCs with combinations of ESC-derived MVs and exosomes for either 1 h (Figure 5A, left panel) or as long as 5 days (Figure 5A, right panel) strongly activated FAK, as determined by western blot analysis using a phospho-FAK-specific antibody. Note that activated FAK was not delivered to ESCs via EVs, as they are devoid of this protein (Figure 1E, top panel). Interestingly, while FAK phosphorylation in ESCs cultured in 2i+LIF medium was determined to be relatively high, it was markedly decreased when the cells were placed in N2B27 medium (Figure 5B), consistent with suggestions that FAK activation is important for maintaining pluripotency (Vitillo et al., 2016; Wrighton et al., 2014). Indeed, we found that treatment of ESCs cultured in 2i+LIF medium with FAK inhibitor III (FAKi) (Figure 5C, top panel) was sufficient to cause the cells to lose the expression of the pluripotent markers Oct3/4 and Nanog (Figure 5C, middle panels) and their ability to form spheres (Figures 5D and 5E). Similar results were obtained when a second FAK inhibitor, Y15 (also sometimes referred to as FAK inhibitor 14), was used (Figures S5A–S5C)

To further examine the role of FAK in maintaining a stem cell phenotype, ESCs were placed in N2B27 differentiation medium containing various combinations of MVs and exosomes isolated from ESCs and treated without or with one of the two FAK inhibitors, FAK inhibitor III (FAKi) or Y15. Again, ESCs treated with EVs retained their ability to form spheres (Figures 5F and S5D, shaded bars) and exhibited AP activity (Figures 5G, S5E, and S5F). However, under conditions where FAK activity was blocked using either of these inhibitors, the number of EV-treated ESCs that retained their sphere-forming ability (Figures 5F and S5D, clear bars) and AP activity (Figures 5G, S5E, and S5F) was significantly reduced. Moreover, the ability of EVs to enable ESCs cultured under differentiation-inducing conditions to maintain their stemness, as determined by Nanog expression, was reduced when FAK activity was inhibited (Figures 5H and S5G). We also determined that ectopically expressing an activated form of FAK, referred to as CD2-FAK (Chan et al., 1994; Shibue and Weinberg, 2009), in ESCs grown in N2B27 medium (Figure S6A) enabled the cells to maintain several of their stem cell phenotypes, including the expression of Oct3/4 and Nanog (Figure S6B), as well as their ability to form spheres (Figure S6C).

Fibronectin Associated with ESC-Derived EVs Is Important for Maintaining Stemness

We examined how ESC-derived EVs activate FAK and found that fibronectin was associated with both MVs and exosomes isolated from ESCs (Figure 6A, lanes labeled 2i+LIF). We also detected fibronectin in the sucrose gradient fractions that contained MVs and exosomes, i.e., in the intermediate-density fractions (Figure 6B). In contrast, the levels of fibronectin detected in the lysates of ESCs that had undergone differentiation and correspondingly in

their shed MVs and exosomes were greatly reduced (Figure 6A, lanes labeled N2B27). When these vesicles were used to treat ESCs undergoing differentiation, they were unable to maintain Oct3/4 and Nanog expression, unlike EVs derived from pluripotent ESCs (Figure 6C, compare lanes 3 and 4). These findings indicate that fibronectin plays a key role in the ability of ESC-derived EVs to maintain stemness.

ESCs cultured in N2B27 medium were then treated with different combinations of EVs, as well as with the RGD peptide, which acts as an antagonist and competes with fibronectin to engage and activate integrins expressed on the surfaces of recipient cells (Ruoslahti and Pierschbacher, 1987). Under conditions where the RGD peptide reduced the levels of activated FAK in cells treated with ESC-derived EVs (Figure 6D), the EVs were much less effective in maintaining the expression of Oct3/4 and Nanog (Figure 6E). We then tested whether fibronectin alone (i.e., soluble fibronectin) or the conditioned medium collected from pluripotent stem cells depleted of MVs and exosomes (i.e., vesicle-free medium; VFM) could recapitulate the effects of the EVs. The relative amount of fibronectin associated with ESC-derived MVs and exosomes used to promote stemness in our experiments was determined by subjecting the EVs, together with increasing amounts of purified fibronectin, to western blot analysis. Figure 6F shows that between 160 and 320 ng of fibronectin was associated with the EV preparations. Thus, ESCs were placed in N2B27 medium containing 320 ng of purified fibronectin. This condition was unable to maintain the expression of Oct3/4 and Nanog in ESCs (Figure 6G, compare lanes 1 and 3) or promote sphere formation (Figures 6H and 6I). Similarly, treatment of ESCs undergoing differentiation with the VFM collected from pluripotent ESCs was markedly less effective in promoting the expression of pluripotency markers in recipient cells, compared to ESC-derived EVs (Figure 6J, compare lanes 3 and 4). However, when an ~15-fold excess (i.e., 5.0 μg) of purified fibronectin over what is typically associated with the EVs from pluripotent ESCs was used to treat ESCs placed in N2B27 medium, the levels of FAK activity as well as Oct3/4 and Nanog expression were increased compared to untreated cells (Figure S6D). These same cells also started to form spheres (Figure S6E), although even this relatively large amount of fibronectin was not nearly as effective at mediating these effects as the EVs from pluripotent ESCs.

We then considered whether the fibronectin associated with the EVs from ESCs was important for their ability to dock onto recipient cells. We used the FM1-43FX fluorescent membrane dye to label the MVs and exosomes produced by pluripotent ESCs and then added the vesicles to cultures of ESCs that had been treated without or with the RGD peptide. Consistent with our earlier findings, the cells treated with only the labeled MVs and exosomes exhibited fluorescence, indicating that the vesicles associated with the ESCs (Figure S7A). Treatment of the cells with the RGD peptide did not change this effect. The MVs and exosomes from ESCs that had undergone differentiation, such that they produced EVs that lacked fibronectin (see Figure 6A), were similarly labeled with FM1-43FX before being used to treat other ESCs. Again, the cells treated with either class of EVs isolated from the differentiated ESCs exhibited fluorescence (Figure S7B), thus indicating that fibronectin associated with EVs from pluripotent ESCs is not required for their ability to dock onto recipient cells. Rather, collectively, our findings suggest that fibronectin, specifically when associated with ESC-derived EVs, is capable of engaging integrins and

stimulating the activation of FAK in ESCs, which then prevents premature differentiation and helps maintain a pluripotent state.

DISCUSSION

Compared to the amount of available information regarding the culturing conditions required to maintain stem cells in an undifferentiated pluripotent state (Evans and Kaufman, 1981; Nishikawa et al., 2007; Thomson et al., 1998; Ying et al., 2008), much less is known about the mechanisms that maintain stemness *in vivo*. This is especially the case for the pluripotent cells that are only transiently present within the epiblast layer of the ICM in blastocysts (Figure 7). If these cells lose their pluripotency too early or if their normal transition from a pluripotent to a differentiated state is delayed, this can have catastrophic effects on embryonic development (Young, 2011). In recent years, the roles that EVs play in several different disease states (Feng et al., 2017; Antonyak et al., 2011) as well as in a growing number of physiological processes (Desrochers et al., 2016a, 2016b) have become increasingly appreciated. We previously showed that ESCs generate MVs that promote the migration of trophoblasts, which has important consequences for a key step during early pregnancy, namely the implantation of the blastocyst into the uterine wall (Desrochers et al., 2016b). Also, there have been suggestions that EVs produced by stem cells can be used for regenerative purposes by promoting the survival and recovery of diseased or damaged cells (Hur et al., 2020; Khan et al., 2015; Rani et al., 2015).

We now demonstrate that EVs shed by ESCs provide a mechanism for intercellular communication that has important consequences for the maintenance of ESC survival and stemness. Furthermore, we show that these actions require fibronectin that is associated with the vesicles, thus enabling them to activate FAK in the ESCs that they engage. Previous studies have shown that fibronectin associates with both MVs and exosomes and that it plays important roles in the ability of EVs to contribute to cancer progression, as well as in the developing embryo where its association with MVs helps to activate trophoblast migration and invasion into the uterine wall (Antonyak et al., 2011; Desrochers et al., 2016b; Jeppesen et al., 2019). Moreover, there have been various reports that integrins and FAK are important for the ability of ESCs to remain viable and maintain their pluripotent state. However, there have also been contradictory reports, in some cases suggesting distinct outcomes for FAK activation on ESC viability and pluripotency (Hayashi et al., 2007; Vitillo et al., 2016; Wrighton et al., 2014). These discrepancies may be due, in part, to the origin of the ESCs (i.e., human versus mouse), their state of pluripotency, and the specific culturing conditions used (Ghimire et al., 2018; Mascetti and Pedersen, 2014; Tesar et al., 2007). For example, there are several distinct states of pluripotency, including naive and primed, that differ in their expression of specific genes, metabolic activity, and developmental potential (Kinoshita and Smith, 2018; Nichols and Smith, 2012; Nichols et al., 2009). ESCs in the naive state most closely resemble the epiblast cells in pre-implantation blastocysts and have the potential to undergo the full range of cell fate transitions essential for organism development. In contrast, stem cells in the primed state represent epiblast cells in post-implantation embryos and have a more limited pluripotent capacity. Several of the findings demonstrating a role for FAK in the promotion of pluripotency involved studies using stem cells that were most likely in the primed state or that represented a mixed population of

pluripotent cells (Vitillo et al., 2016; Wrighton et al., 2014; Hayashi et al., 2007). Here, we show that upon engaging ESCs cultured under conditions that normally promote their differentiation, EVs shed from mouse ESCs in a naive state activate FAK and enable the cells to maintain their stem cell phenotypes; although at present, we cannot definitively determine whether the treated ESCs were also in a naive or a primed state.

The ability of ESC-derived EVs to maintain pluripotency is dependent on fibronectin that is associated with the surfaces of these vesicles. The EV-associated fibronectin is more effective at stimulating FAK activity within ESCs compared to when these cells are treated with fibronectin in the absence of vesicles. This is reminiscent of our earlier finding that MVs containing bound VEGF were much more effective at stimulating VEGF receptors on endothelial cells compared to free VEGF (Feng et al., 2017). The ability of ESCs to generate and release large numbers of EVs, each of which has multiple associated fibronectin molecules, could provide a mechanism for multivalent interactions between EV-associated fibronectin and integrins on the surfaces of the targeted ESCs. This would be expected to significantly increase the potency of FAK activation and thereby provide a strong signaling cue for maintaining stem cell phenotypes, i.e., the ability to form spheres, exhibit enhanced AP activity, and express pluripotent markers. It is also possible that additional EV cargo works together with EV-associated fibronectin to help maintain stemness and the pluripotent state. Although we initially suspected that these effects might be mediated by the transfer of EV-associated RNA transcripts encoding several pluripotent transcription factors, we, in fact, detected very little RNA in MVs isolated from the ESCs. In the case of ESC-derived exosomes, the RNA transcripts encoding pluripotent factors associated with these EVs were degraded by treatment with RNase A, without any functional consequences.

ESCs are actively being pursued for therapeutic applications, especially in the context of regenerative medicine. The idea is that these pluripotent cells will replace damaged and diseased tissues (Murry and Keller, 2008; Tabar and Studer, 2014). To achieve such a goal, there has been a great deal of research effort aimed at understanding the regulatory cues that enable ESCs to maintain their pluripotent state and, at the appropriate time, induce their differentiation to a specific cell lineage. Our findings now describe a mechanism for intercellular communication between pluripotent cells within the epiblast, which might shed new light on how this regulation is achieved. As depicted in Figure 7, the shedding of fibronectin-associated EVs could help to ensure that ESCs remain viable and maintain their pluripotent state until the proper time when they receive dominant signals from their surroundings to undergo differentiation and transition to specific cellular lineages. Interestingly, we have found that ESCs, upon their differentiation, also produce large quantities of MVs and exosomes. Moreover, the EVs derived from these differentiated cells lack associated fibronectin. Therefore, an intriguing possibility, which we plan to test in the future, is that EVs derived from differentiated cells in the proximity of pluripotent cells serve as a signaling cue for driving their differentiation. These, and other related studies, should contribute to a broader understanding of how ESCs undergo cell fate transitions as well as potentially highlighting new strategies for enhancing the efficiency of stem cell therapy.

STAR★METHODS

RESOURCE AVAILABILITY

Lead Contact—Further information and requests for reagents may be directed to and will be fulfilled by the Lead Contact, Richard Cerione (rac1@cornell.edu).

Materials Availability—This study did not generate new unique reagents.

Data and Code Availability—Original data are deposited in Mendeley Data: http://doi.org/10.17632/mt4gm74tbw.1

EXPERIMENTAL MODEL AND SUBJECT DETAILS

Cell Lines—E14tg2a.4 mouse embryonic stem cells (ESCs) were cultured on 0.1% gelatin-coated plates in a 1:1 mixture of DMEM/F12 and Neurobasal medium supplemented with N-2 Supplement (100X, Thermo Fisher Scientific), B27 Supplement (50X, Thermo Fisher Scientific), 0.05% bovine serum albumin (BSA), 2 mM glutamine, 1 μM PD03259010, 3 μM CHIR99021, 1.5 x 10^{-4} M Monothioglycerol, and 1,000 units/ml leukemia inhibitory factor (LIF). This medium is referred to as 2i+LIF medium. v6.5 mouse ESCs were cultured on 0.1% gelatin-coated plates containing mouse embryonic fibroblast (MEF) feeder cells, in 2i+LIF medium. MEFs were cultured on 0.1% gelatin-coated plates in DMEM medium supplemented with 10% fetal bovine serum. All cells were maintained at 37°C in a humidified atmosphere containing 5% CO_2.

METHOD DETAILS

ESC Differentiation—ESCs were plated at a density of 0.5 x 10^4 cells/cm^2 on 0.1% gelatin-coated plates, and cultured in a 1:1 mixture of DMEM/F12 and Neurobasal medium supplemented with N-2 Supplement, B27 Supplement, 7.5% BSA, 2 mM glutamine, and 1.5x10^{-4} M Monothioglycerol. This medium is referred to as N2B27 medium. The medium was replaced daily for up to 5 days.

Inhibitor and Purified Fibronectin Treatments—Cells maintained under the indicated culturing conditions were treated with 7.5 μM FAK inhibitor III (FAKi), 2.5 μM Y15 (also referred to as FAK inhibitor 14), 25 μg/ml RGD peptide, and either 320 ng or 5.0 μg of purified fibronectin. An equivalent volume of vehicle control (i.e. DMSO for the FAK inhibitor III, and water for the RGD-peptide, Y15, and purified fibronectin) was added to the untreated control groups.

Transfections—ESCs were either mock transfected, or were transfected with a plasmid encoding an activated form of FAK, pLV-neo-CD2-FAK (Addgene, #37013; a gift from Dr. Robert Weinberg, Whitehead Institute, MIT), using Lipofectamine with PLUS Reagent (Thermo Fisher Scientific) according to the manufacturer's instructions.

EV and Vesicle Free Medium (VFM) Collection—The conditioned medium collected from two 150 mm plates of ESCs containing ~8.0 x 10^7 cells, and cultured under the indicated conditions, was centrifuged twice at 1,000 x g for 5 minutes to pellet cells and

debris. The partially clarified medium was then filtered using a 0.22 μm Steriflip filter unit (Millipore), and the filter was washed with 10 ml of phosphate buffered saline (PBS). The EVs retained by the filter (i.e. those larger than 0.22 μm) were considered microvesicles (MVs), and were either resuspended in PBS for use primarily in biological assays, or lysed using lysis buffer (25 mM Tris, 100 mM NaCl, 1% Triton X-100, 1 mM EDTA, 1 mM DTT, 1 mM $NaVO_4$, 1 mM β-glycerol phosphate, 1 μg/ml aprotinin, and 1 μg/ml leupeptin). The filtrate was subjected to ultracentrifugation at 100,0 x g for 2.5 hours using a Type 45 Ti rotor to pellet the EVs smaller than 0.22 μm (i.e. exosomes). The pelleted exosomes were either resuspended in PBS or lysed using lysis buffer. The resulting supernatant depleted of MVs and exosomes was concentrated using 100 KDa cut-off Centricon units (Amicon), and was considered the vesicle-free medium (VFM).

Sucrose Gradient—Isolated MVs and exosomes resuspended in PBS as described above were moved to ultra-clear SW 41 tubes (Beckman Coulter), combined with 1.5 ml of a 2.5 M sucrose solution, and mixed gently by vortexing for 5 seconds. A linear sucrose gradient was assembled on top of the mixture by sequentially layering 700 μl of 15 fractions (i.e. sucrose molarity of each fraction: 2.0 M, 1.886 M, 1.771 M, 1.657 M, 1.543 M, 1.429 M, 1.314 M, 1.200 M, 1.086 M, 0.971 M, 0.857 M, 0.743 M, 0.629 M, 0.514 M, 0.400 M). The sucrose gradients were then subjected to ultracentrifugation at 192,000 x g for 17 hours using an SW 41 Ti rotor. Twelve 1 ml gradient fractions were collected and pooled together in groups of four, representing low-, intermediate-, and high-density fractions. The pooled fractions were mixed with PBS, placed in ultra-clear SW 41 tubes, and ultracentrifuged using an SW 41 Ti rotor at 100,000 x g for 70 minutes. The resulting vesicle pellets were lysed with lysis buffer.

Nanoparticle Tracking Analysis (NTA)—The sizes and concentrations of EVs in a given sample were determined using a NanoSight NS300 (Malvern, Cornell NanoScale Science and Technology Facility) as described previously in Kreger et al. (2016). Briefly, the conditioned medium collected from cultures of ESCs was centrifuged twice at 1,000 x g for 5 minutes to pellet cells and debris. The partially clarified medium was then diluted in PBS and injected into the beam path to capture movies of EVs as points of diffracted light moving rapidly under Brownian motion. Five 45-second videos of each sample were taken and analyzed to determine the concentration and size of the individual EVs based on their movement, and then results were averaged together.

Labeling EVs with FM1-43FX Dye—The conditioned medium collected from two 150 mm plates of pluripotent or differentiated ESCs containing ~8.0 x 10^7 cells was centrifuged twice at 1,000 ~ g for 5 minutes to pellet cells and cell debris. FM1-43FX dye (Thermo Fisher Scientific) was then added to the partially clarified medium to a final concentration of 5 μg/ml for 30 minutes. The MVs and exosomes were then isolated from the conditioned medium using the filtration and the ultracentrifugation approach described, which removes any soluble (i.e. unincorporated) dye. To show the transfer of EVs to recipient ESCs, MVs or exosomes labeled with FM1-43FX dye were added to ESCs. After a 1 hour incubation, the cells were washed three times with PBS, stained with DAPI to label nuclei, and fixed with 4% formaldehyde in PBS for 10 minutes. The cells were then washed three times with

PBS, mounted, and visualized using brightfield and fluorescent microscopy. All images were captured using IPLABS software and processed using ImageJ software.

Negative Stain Electron Microscopy—10 μl of the conditioned medium collected from cultures of ESCs was pipetted onto a copper grid, incubated for 2 minutes, and the excess medium was removed by blotting with filter paper. 10 μl of 2% uranyl acetate was then applied to the grid twice for 30 seconds, at which point blotting with filter paper was used to remove excess liquid. The grid was air-dried for 5 minutes and visualized by electron microscopy.

Western Blot/Immunoblot Analysis—Protein concentrations of cell, MV, and exosome lysates were determined using the Bio-Rad protein assay (Bio-Rad). The lysates were normalized based on protein concentration, resolved by SDS-PAGE, and then transferred to PVDF membranes. The membranes were blocked with 10% BSA in 20 mM Tris, 135 mM NaCl, and 0.02% Tween 20 (TBST) for 30 minutes, and then incubated with the indicated primary antibodies diluted in TBST overnight. After extensive washing with TBST, the membranes were incubated with HRP-conjugated secondary antibodies (Cell Signaling Technology) diluted in TBST for 1 hour, at which point the membranes were washed again with TBST, and exposed to ECL reagent.

Sphere Formation Assay—ESCs were plated in 12 well plates at a density of 20,000 cells/well (i.e. 0.5 x $10^4/cm^2$ density), and cultured in 2i+LIF, or N2B27, medium supplemented with various combinations of MVs, exosomes, FAK inhibitor III (FAKi), Y15, RGD peptide, vesicle free medium (VFM), and purified fibronectin (320 ng or 5.0 μg, as indicated). The medium was replaced daily for 3 days, at which point the cells were passaged, plated again in 6 well ultra-low attachment plates at a density of 20,000 cells/well, and maintained in 2i+LIF medium. MEFs were also plated in ultra-low attachment plates and cultured in the same condition. Two days later, the cells were visualized by brightfield microscopy, and the number of spheres formed was determined. In some cases, the ESCs grown under these conditions were passaged for additional five passages.

Alkaline Phosphatase (AP) Activity Assay—Cells grown in suspension or attached to a plate were incubated with VECTOR Red Alkaline Phosphatase Substrate solution (Vector Laboratories) according to the manufacturer's instructions. After washing the cells with wash buffer (150 mM Tris, pH 8.2, 0.1% Tween 20), the cells were mounted and visualized by brightfield microscopy.

Cell Growth Assay—ESCs were plated in 12 well plates at a density of 20,000 cells/well (i.e. 0.5 x $10^4/cm^2$ density), and cultured in 2i+LIF, or N2B27, medium supplemented with PBS (as a control) or an equivalent amount of MVs and/or exosomes isolated from pluripotent ESCs and resuspended in PBS. The medium was replaced daily for 3 days, at which point the cells in each well were counted.

Cell Death Assay—ESCs were plated in 12 well plates at a density of 20,000 cells/well (i.e. 0.5 x $10^4/cm^2$ density), and cultured in 2i+LIF, or N2B27, medium supplemented with PBS (as a control) or an equivalent amount of MVs and/or exosomes isolated from

pluripotent ESCs and resuspended in PBS. The medium was replaced daily for 3 days, at which point the cells were passaged and plated again in 12 well plates at a density of 20,000 cells/well. Two days later, the cells were trypsinized, incubated with 0.4% Trypan Blue (Thermo Fisher Scientific), and visualized by brightfield microscopy. The percentage of non-viable cells to viable cells was determined for each condition assayed.

Immunofluorescence Microscopy—Cells and blastocysts were plated on 0.1% gelatin-coated chamber slides (Thermo Fisher Scientific), treated as indicated, and then fixed with 3.7% formaldehyde diluted in PBS for 30 minutes. The slides were permeabilized with 0.1% Triton X-100 diluted in PBS, blocked with 10% BSA diluted in PBS, and incubated with an Oct3/4 antibody (Santa Cruz Biotechnology) and a Nanog antibody (Abcam) diluted in 5% BSA in PBS at a 1:200 dilution, for 2 hours. The slides were washed with PBS, and then were incubated with an anti-mouse IgG-Alexa 488 conjugate antibody (Thermo Fisher Scientific) and an anti-rabbit IgG-Alexa 548 conjugate antibody (Thermo Fisher Scientific) diluted in 5% BSA in PBS at a 1:400 dilution, for 1 hour. The slides were again washed with PBS and visualized by brightfield and fluorescent microscopy. All images were captured using IPLABS software (BD Biosciences) and processed using ImageJ software.

Embryo Collection and Blastocyst Outgrowth Assays—Female FVB/N mice, between 8 and 20 weeks of age (Jackson Laboratory), were super-ovulated by injecting pregnant mare's serum gonadotropin (PMSG) and human chorionic gonadotropin (HCG). After mating, post-coital day 0.5 female mice were euthanized, and their uteri were removed. The uteri were flushed with M2 medium to remove embryos, which were then placed in 200 μl of KSOM medium covered by mineral oil for 4 days. The embryos that developed into blastocysts were isolated and placed in 8 well chamber slides (Thermo Fisher Scientific) coated with 0.1% gelatin, and cultured in N2B27 medium supplemented without or with EVs isolated from ESCs, for 5 days. The blastocysts that attached to the slide and spread were fixed, stained for Oct3/4 and Nanog, and visualized by brightfield and fluorescent microscopy.

Signaling Experiments in ESCs—ESCs were placed in 12 well plates at a density of 20,000 cells/well, and cultured in N2B27 medium supplemented with PBS or an equivalent amount of MVs and/or exosomes isolated from pluripotent ESCs for different amounts of time, at which point they were lysed using lysis buffer. The resulting lysates were subjected to immunoblot analysis.

Karyotyping—ESCs cultured in 2i+LIF medium were incubated with colcemid (0.1 μg/ml final concentration) for 2 hours at 37°C. The cells were trypsinized and pelleted by centrifugation at 300 x g for 5 minutes, and the supernatant was removed. 10 ml of 37°C 0.075 M KCl was added drop-by-drop with gentle agitation, followed by the addition of 10 ml of KCl, again with gentle agitation. After incubating the solution at 37°C for 25 minutes, 4-5 drops of fixative (a 3:1 mixture of methyl alcohol and glacial acetic acid) were added to the solution, and the cells were pelleted by centrifugation at 300 x g for 5 minutes. The supernatant was removed, and 10 ml of fixative was added to the pelleted cells. After resuspending the cells using gentle agitation, the solution was centrifuged again at 300 x g

for 5 minutes, and the cell pellet was resuspended with fixative, dropped on a slide glass, and visualized by fluorescence microscopy. All images were captured using IPLABS software and processed using ImageJ software.

RNA Isolation + RT-PCR—Total RNA was isolated from ESCs and EV preparations using the Qiagen RNeasy Mini kit (Qiagen), and the mRNA transcripts were converted to cDNA using Superscript III Reverse Transcriptase (Invitrogen) and oligo dT_{20}. The concentration of cDNA was measured using a NanoDrop Spectrophotometer (Thermo Fisher Scientific), and the cDNA samples were subjected to RT-PCR

ESC Microinjection into Mouse Blastocysts—Female B6(Cg)-*Tyr*$^{c\text{-}2J}$/J (B6-albino) mice, between 8 and 20 weeks of age (Jackson Laboratory), were super-ovulated by injecting pregnant mare's serum gonadotropin (PMSG) and human chorionic gonadotropin (HCG). After mating, post-coital day 3.5 female mice were euthanized, and their uteri were removed and flushed with M2 medium to obtain blastocysts. At the same time, the v6.5 ESC line derived from C57BL/6 X 129/sv mice was plated in 60 mm dishes (without a fibroblast feeder layer) at a density of 1.47 x 10^6 cells/dish (i.e. 0.7 x 10^5/cm^2 density), and cultured in 2i+LIF medium, N2B27 medium, or N2B27 medium supplemented with MVs and exosomes from E14tg2a.4 ESCs. Thirty hours later, the cells were trypsinized, and then individual cells were injected into the collected blastocysts. The blastocysts were then surgically transferred into the uterine horns of pseudopregnant recipient females. Typically, 3 weeks later, pups were born and allowed to develop their coat. When the injected cells successfully integrated into the embryos, the resulting pups were chimeras, which had patches of coat color from both the host embryo (white) and the injected cells (black), while the pups derived from the blastocysts without ESC integration exhibited only white coat color.

QUANTIFICATION AND STATISTICAL ANALYSIS

Quantitative data are presented as means ± SD. All experiments were independently performed at least three times. Statistical significance of the experiments was determined using Student's t-tests; ****; $p < 0.0001$, ***; $p < 0.001$, **; $p < 0.01$, *; $p < 0.05$, and ns; not significant. Statistical analysis was performed in GraphPad PRISM 7.

Supplementary Material

Refer to Web version on PubMed Central for supplementary material.

ACKNOWLEDGMENTS

We thank Cindy Westmiller for helping to prepare the manuscript. We acknowledge Robert Munroe and Christian Abratte at Cornell's Stem Cell and Transgenic Core Facility for their expertise in isolating blastocysts and carrying out the experiments involving animal models. This work was supported by the National Institutes of Health grants (GM122575 and CA201402).

REFERENCES

Abranches E, Silva M, Pradier L, Schulz H, Hummel O, Henrique D, and Bekman E (2009). Neural differentiation of embryonic stem cells in vitro: a road map to neurogenesis in the embryo. PLoS One 4, e6286, 10.1371/journal.pone.0006286. [PubMed: 19621087]

Andreu Z, and Yáñez-Mó M (2014). Tetraspanins in extracellular vesicle formation and function. Front. Immunol 5, 442, 10.3389/fimmu.2014.00442. [PubMed: 25278937]

Antonyak MA, and Cerione RA (2014). Microvesicles as mediators of intercellular communication in cancer. Methods Mol. Biol 1165, 147–173. [PubMed: 24839024]

Antonyak MA, Li B, Boroughs LK, Johnson JL, Druso JE, Bryant KL, Holowka DA, and Cerione RA (2011). Cancer cell-derived microvesicles induce transformation by transferring tissue transglutaminase and fibronectin to recipient cells. Proc. Natl. Acad. Sci. USA 108, 4852–4857. [PubMed: 21368175]

Beddington RSP, and Robertson EJ (1989). An assessment of the developmental potential of embryonic stem cells in the midgestation mouse embryo. Development 105, 733–737. [PubMed: 2598811]

Boland MJ, Nazor KL, and Loring JF (2014). Epigenetic regulation of pluripotency and differentiation. Circ. Res 115, 311–324. [PubMed: 24989490]

Chambers I, Colby D, Robertson M, Nichols J, Lee S, Tweedie S, and Smith A (2003). Functional expression cloning of Nanog, a pluripotency sustaining factor in embryonic stem cells. Cell 113, 643–655. [PubMed: 12787505]

Chan PY, Kanner SB, Whitney G, and Aruffo A (1994). A transmembrane-anchored chimeric focal adhesion kinase is constitutively activated and phosphorylated at tyrosine residues identical to pp125FAK. J. Biol. Chem 269, 20567–20574. [PubMed: 8051157]

Costa-Silva B, Aiello NM, Ocean AJ, Singh S, Zhang H, Thakur BK, Becker A, Hoshino A, Mark MT, Molina H, et al. (2015). Pancreatic cancer exosomes initiate pre-metastatic niche formation in the liver. Nat. Cell Biol 17, 816–826. [PubMed: 25985394]

DeChiara TM, Poueymirou WT, Auerbach W, Frendewey D, Yancopoulos GD, and Valenzuela DM (2010). Producing fully ES cell-derived mice from eight-cell stage embryo injections. Methods Enzymol 476, 285–294. [PubMed: 20691872]

Desrochers LM, Antonyak MA, and Cerione RA (2016a). Extracellular vesicles: satellites of information transfer in cancer and stem cell biology. Dev. Cell 37, 301–309. [PubMed: 27219060]

Desrochers LM, Bordeleau F, Reinhart-King CA, Cerione RA, and Antonyak MA (2016b). Microvesicles provide a mechanism for intercellular communication by embryonic stem cells during embryo implantation. Nat. Commun 7, 11958, 10.1038/ncomms11958. [PubMed: 27302045]

Dodge JE, Kang YK, Beppu H, Lei H, and Li E (2004). Histone H3-K9 methyltransferase ESET is essential for early development. Mol. Cell. Biol 24, 2478–2486. [PubMed: 14993285]

Evans MJ, and Kaufman MH (1981). Establishment in culture of pluripotential cells from mouse embryos. Nature 292, 154–156. [PubMed: 7242681]

Feng Q, Zhang C, Lum D, Druso JE, Blank B, Wilson KF, Welm A, Antonyak MA, and Cerione RA (2017). A class of extracellular vesicles from breast cancer cells activates VEGF receptors and tumour angiogenesis. Nat. Commun 8, 14450, 10.1038/ncomms14450. [PubMed: 28205552]

Gardner RL, and Cockroft DL (1998). Complete dissipation of coherent clonal growth occurs before gastrulation in mouse epiblast. Development 125, 2397–2402. [PubMed: 9609822]

Ghimire S, Van Der Jeught M, Neupane J, Roost MS, Anckaert J, Popovic M, Van Nieuwerburgh F, Mestdagh P, Vandesompele J, Deforce D, et al. (2018). Comparative analysis of naive, primed and ground state pluripotency in mouse embryonic stem cells originating from the same genetic background. Sci. Rep 8, 5884, 10.1038/s41598-018-24051-5. [PubMed: 29650979]

Hayashi Y, Furue MK, Okamoto T, Ohnuma K, Myoishi Y, Fukuhara Y, Abe T, Sato JD, Hata R-I, and Asashima M (2007). Integrins regulate mouse embryonic stem cell self-renewal. Stem Cells 25, 3005–3015. [PubMed: 17717067]

Hu M, Wei H, Zhang J, Bai Y, Gao F, Li L, and Zhang S (2013). Efficient production of chimeric mice from embryonic stem cells injected into 4- to 8-cell and blastocyst embryos. J. Anim. Sci. Biotechnol 4, 12, 10.1186/2049-1891-4-12. [PubMed: 23514327]

Hur YH, Cerione RA, and Antonyak MA (2020). Extracellular vesicles and their roles in stem cell biology. Stem Cells 88, 469–476.

Jeppesen DK, Fenix AM, Franklin JL, Higginbotham JN, Zhang Q, Zimmerman LJ, Liebler DC, Ping J, Liu Q, Evans R, et al. (2019). Reassessment of exosome composition. Cell 177, 428–445.e18. [PubMed: 30951670]

Juan AH, Wang S, Ko KD, Zare H, Tsai PF, Feng X, Vivanco KO, Ascoli AM, Gutierrez-Cruz G, Krebs J, et al. (2016). Roles of H3K27me2 and H3K27me3 examined during fate specification of embryonic stem cells. Cell Rep. 18, 1369–1382, 10.1016/j.celrep.2016.12.036.

Kashyap V, Rezende NC, Scotland KB, Shaffer SM, Persson JL, Gudas LJ, and Mongan NP (2009). Regulation of stem cell pluripotency and differentiation involves a mutual regulatory circuit of the Nanog, OCT4, and SOX2 pluripotency transcription factors with polycomb repressive complexes and stem cell microRNAs. Stem Cells Dev. 18, 1093–1108. [PubMed: 19480567]

Katsman D, Stackpole EJ, Domin DR, and Farber DB (2012). Embryonic stem cell-derived microvesicles induce gene expression changes in Müller cells of the retina. PLoS One 7, e50417, 10.1371/journal.pone.0050417. [PubMed: 23226281]

Khan M, Nickoloff E, Abramova T, Johnson J, Verma SK, Krishnamurthy P, Mackie AR, Vaughan E, Garikipati VNS, Benedict C, et al. (2015). Embryonic stem cell-derived exosomes promote endogenous repair mechanisms and enhance cardiac function following myocardial infarction. Circ. Res 117, 52–64. [PubMed: 25904597]

Kinoshita M, and Smith A (2018). Pluripotency deconstructed. Dev. Growth Differ 60, 44–52. [PubMed: 29359419]

Kreger BT, Johansen ER, Cerione RA, and Antonyak MA (2016). The enrichment of survivin in exosomes from breast cancer cells treated with paclitaxel promotes cell survival and chemoresistance. Cancers (Basel) 8, 111, 10.3390/cancers8120111.

Latifkar A, Hur YH, Sanchez JC, Cerione RA, and Antonyak MA (2019). New insights into extracellular vesicle biogenesis and function. J. Cell Sci 132, 10.1242/jcs.222406.

Li B, Antonyak MA, Zhang J, and Cerione RA (2012). RhoA triggers a specific signaling pathway that generates transforming microvesicles in cancer cells. Oncogene 31, 4740–4749. [PubMed: 22266864]

Mascetti VL, and Pedersen RA (2014). Naiveté of the human pluripotent stem cell. Nat. Biotechnol 32, 68–70. [PubMed: 24406934]

Mitsui K, Tokuzawa Y, Itoh H, Segawa K, Murakami M, Takahashi K, Maruyama M, Maeda M, and Yamanaka S (2003). The homeoprotein nanog is required for maintenance of pluripotency in mouse epiblast and ES cells. Cell 113, 631–642. [PubMed: 12787504]

Murry CE, and Keller G (2008). Differentiation of embryonic stem cells to clinically relevant populations: lessons from embryonic development. Cell 132, 661–680. [PubMed: 18295582]

Nichols J, Silva J, Roode M, and Smith A (2009). Suppression of Erk signalling promotes ground state pluripotency in the mouse embryo. Development 136, 3215–3222. [PubMed: 19710168]

Nichols J, and Smith A (2012). Pluripotency in the embryo and in culture. Cold Spring Harb. Perspect. Biol 4, a008128, 10.1101/cshperspect.a008128. [PubMed: 22855723]

Nichols J, Zevnik B, Anastassiadis K, Niwa H, Klewe-Nebenius D, Chambers I, Schöler H, and Smith A (1998). Formation of pluripotent stem cells in the mammalian embryo depends on the POU transcription factor Oct4. Cell 95, 379–391. [PubMed: 9814708]

Nishikawa SI, Jakt LM, and Era T (2007). Embryonic stem-cell culture as a tool for developmental cell biology. Nat. Rev. Mol. Cell Biol 8, 502–507. [PubMed: 17522593]

O'Carroll D, Erhardt S, Pagani M, Barton SC, Surani MA, and Jenuwein T (2001). The polycomb-group geneEzh2 is required for early mouse development. Mol. Cell. Biol 21, 4330–4336. [PubMed: 11390661]

Pastrana E, Silva-Vargas V, and Doetsch F (2011). Eyes wide open: a critical review of sphere-formation as an assay for stem cells. Cell Stem Cell 8, 486–498. [PubMed: 21549325]

Petruk S, Cai J, Sussman R, Sun G, Kovermann SK, Mariani SA, Calabretta B, McMahon SB, Brock HW, Iacovitti L, et al. (2017). Delayed accumulation of H3K27me3 on nascent DNA is essential for recruitment of transcription factors at early stages of stem cell differentiation. Mol. Cell 66, 247–257.e5. [PubMed: 28410996]

Rani S, Ryan AE, Griffin MD, and Ritter T (2015). Mesenchymal stem cell-derived extracellular vesicles: toward cell-free therapeutic applications. Mol. Ther 23, 812–823. [PubMed: 25868399]

Ratajczak J, Miekus K, Kucia M, Zhang J, Reca R, Dvorak P, and Ratajczak MZ (2006). Embryonic stem cell-derived microvesicles reprogram hematopoietic progenitors: evidence for horizontal transfer of mRNA and protein delivery. Leukemia 20, 847–856. [PubMed: 16453000]

Rege TA, and Hagood JS (2006). Thy-1, a versatile modulator of signaling affecting cellular adhesion, proliferation, survival, and cytokine/growth factor responses. Biochim. Biophys. Acta 1763, 991–999. [PubMed: 16996153]

Ruoslahti E, and Pierschbacher MD (1987). New perspectives in cell adhesion: RGD and integrins. Science 238, 491–497. [PubMed: 2821619]

Shibue T, and Weinberg RA (2009). Integrin β1-focal adhesion kinase signaling directs the proliferation of metastatic cancer cells disseminated in the lungs. Proc. Natl. Acad. Sci. USA 106, 10290–10295. [PubMed: 19502425]

Snow MHL (1977). Gastrulation in the mouse: growth and regionalization of the epiblast. J. Embryol. Exp. Morphol 42, 293–303.

Surani MA, Hayashi K, and Hajkova P (2007). Genetic and epigenetic regulators of pluripotency. Cell 128, 747–762. [PubMed: 17320511]

Tabar V, and Studer L (2014). Pluripotent stem cells in regenerative medicine: challenges and recent progress. Nat. Rev. Genet 15, 82–92. [PubMed: 24434846]

Tachibana M, Sugimoto K, Nozaki M, Ueda J, Ohta T, Ohki M, Fukuda M, Takeda N, Niida H, Kato H, et al. (2002). G9a histone methyltransferase plays a dominant role in euchromatic histone H3 lysine 9 methylation and is essential for early embryogenesis. Genes Dev 16, 1779–1791. [PubMed: 12130538]

Takahashi K, Tanabe K, Ohnuki M, Narita M, Ichisaka T, Tomoda K, and Yamanaka S (2007). Induction of pluripotent stem cells from adult human fibroblasts by defined factors. Cell 131, 861–872. [PubMed: 18035408]

Takahashi K, and Yamanaka S (2006). Induction of pluripotent stem cells from mouse embryonic and adult fibroblast cultures by defined factors. Cell 126, 663–676. [PubMed: 16904174]

Tamm C, Pijuan Galitó SP, and Annerén C (2013). A comparative study of protocols for mouse embryonic stem cell culturing. PLoS One 8, e81156, 10.1371/journal.pone.0081156. [PubMed: 24339907]

Tesar PJ, Chenoweth JG, Brook FA, Davies TJ, Evans EP, Mack DL, Gardner RL, and McKay RDG (2007). New cell lines from mouse epiblast share defining features with human embryonic stem cells. Nature 448, 196–199. [PubMed: 17597760]

Thomson JA, Itskovitz-Eldor J, Shapiro SS, Waknitz MA, Swiergiel JJ, Marshall VS, and Jones JM (1998). Embryonic stem cell lines derived from human blastocysts. Science 282, 1145–1147. [PubMed: 9804556]

Thomson M, Liu SJ, Zou LN, Smith Z, Meissner A, and Ramanathan S (2011). Pluripotency factors in embryonic stem cells regulate differentiation into germ layers. Cell 145, 875–889. [PubMed: 21663792]

Valadi H, Ekström K, Bossios A, Sjöstrand M, Lee JJ, and Lötvall JO (2007). Exosome-mediated transfer of mRNAs and microRNAs is a novel mechanism of genetic exchange between cells. Nat. Cell Biol 9, 654–659. [PubMed: 17486113]

Van Niel G, D'Angelo G, and Raposo G (2018). Shedding light on the cell biology of extracellular vesicles. Nat. Rev. Mol. Cell Biol 19, 213–228. [PubMed: 29339798]

Vitillo L, Baxter M, Iskender B, Whiting P, and Kimber SJ (2016). Integrin-associated focal adhesion kinase protects human embryonic stem cells from apoptosis, detachment, and differentiation. Stem Cell Rep. 7, 167–176.

Willms E, Cabañas C, Mäger I, Wood MJA, and Vader P (2018). Extracellular vesicle heterogeneity: subpopulations, isolation techniques, and diverse functions in cancer progression. Front. Immunol 9, 738, 10.3389/fimmu.2018.00738. [PubMed: 29760691]

Wrighton PJ, Klim JR, Hernandez BA, Koonce CH, Kamp TJ, and Kiessling LL (2014). Signals from the surface modulate differentiation of human pluripotent stem cells through glycosaminoglycans and integrins. Proc. Natl. Acad. Sci. USA 111, 18126–18131. [PubMed: 25422477]

Ying QL, Wray J, Nichols J, Batlle-Morera L, Doble B, Woodgett J, Cohen P, and Smith A (2008). The ground state of embryonic stem cell self-renewal. Nature 453, 519–523. [PubMed: 18497825]

Young RA (2011). Control of the embryonic stem cell state. Cell 144, 940–954. [PubMed: 21414485]

Highlights

- Maintenance of embryonic stem cell pluripotency is a tightly regulated process
- Extracellular vesicles produced by embryonic stem cells help maintain pluripotency
- Fibronectin bound to extracellular vesicles plays an essential role in their function
- Embryonic stem-cell-derived extracellular vesicles activate FAK to maintain pluripotency

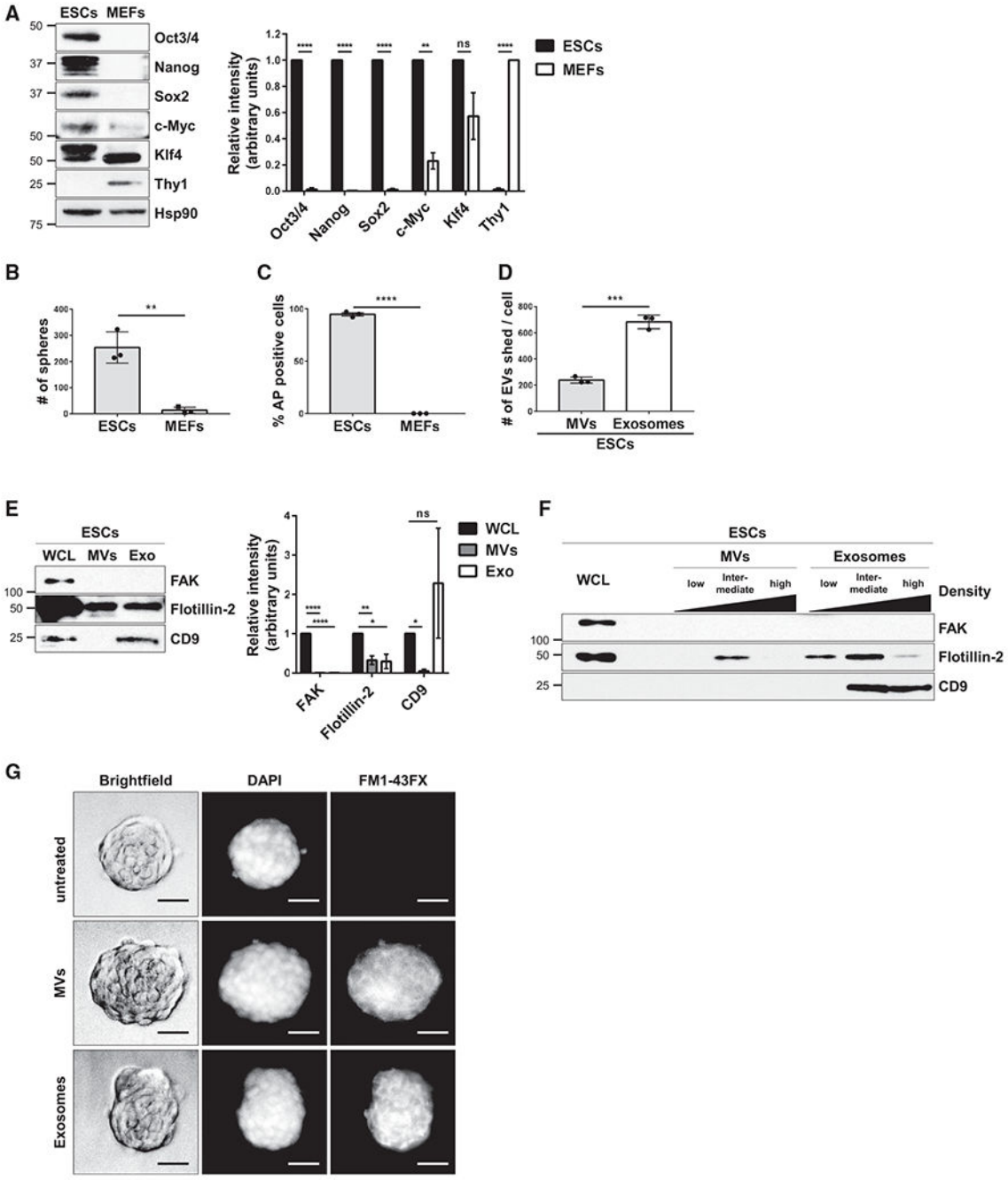

Figure 1. ESCs Generate EVs

(A) ESCs and MEFs were immunoblotted for markers of pluripotency (i.e., Oct3/4, Nanog, Sox2, c-Myc, and Klf4), the fibroblast marker Thy1, and heat shock protein 90 (Hsp90) as the loading control.*

(B) Sphere formation assays were performed on ESCs and MEFs. See corresponding images in Figure S1C.*

(C) AP activity assays were performed on ESCs and MEFs. See corresponding images in Figure S1E.*

(D) The number of MVs and exosomes released per ESC were determined using nanoparticle tracking analysis (NTA).*

(E) ESCs (whole cell lysate; WCL), MVs, and exosomes (Exo) were immunoblotted for the cytosolic protein FAK, the general EV marker Flotillin-2, and the exosome-specific marker CD9.*

(F) MVs and exosomes isolated from ESCs were further subjected to sucrose density gradient ultracentrifugation. ESCs (WCL) and the resulting fractions were immunoblotted for the same proteins described in (E).

(G) MVs and exosomes from ESCs that had been labeled with the fluorescent membrane dye FM1-43FX were incubated with cultures of ESCs for 1 h, at which point the cells were washed extensively, fixed, and stained with DAPI to label nuclei. Brightfield and fluorescent microscopy images of the assay are shown. Scale bar, 50 μm.

*The data shown in (A)–(E) are presented as mean ± SD. All experiments were performed at least three independent times, and statistical significance was determined using Student's t test; ****$p < 0.0001$; ***$p < 0.001$; **$p < 0.01$; *$p < 0.05$; and ns, not significant. See also Figure S1.

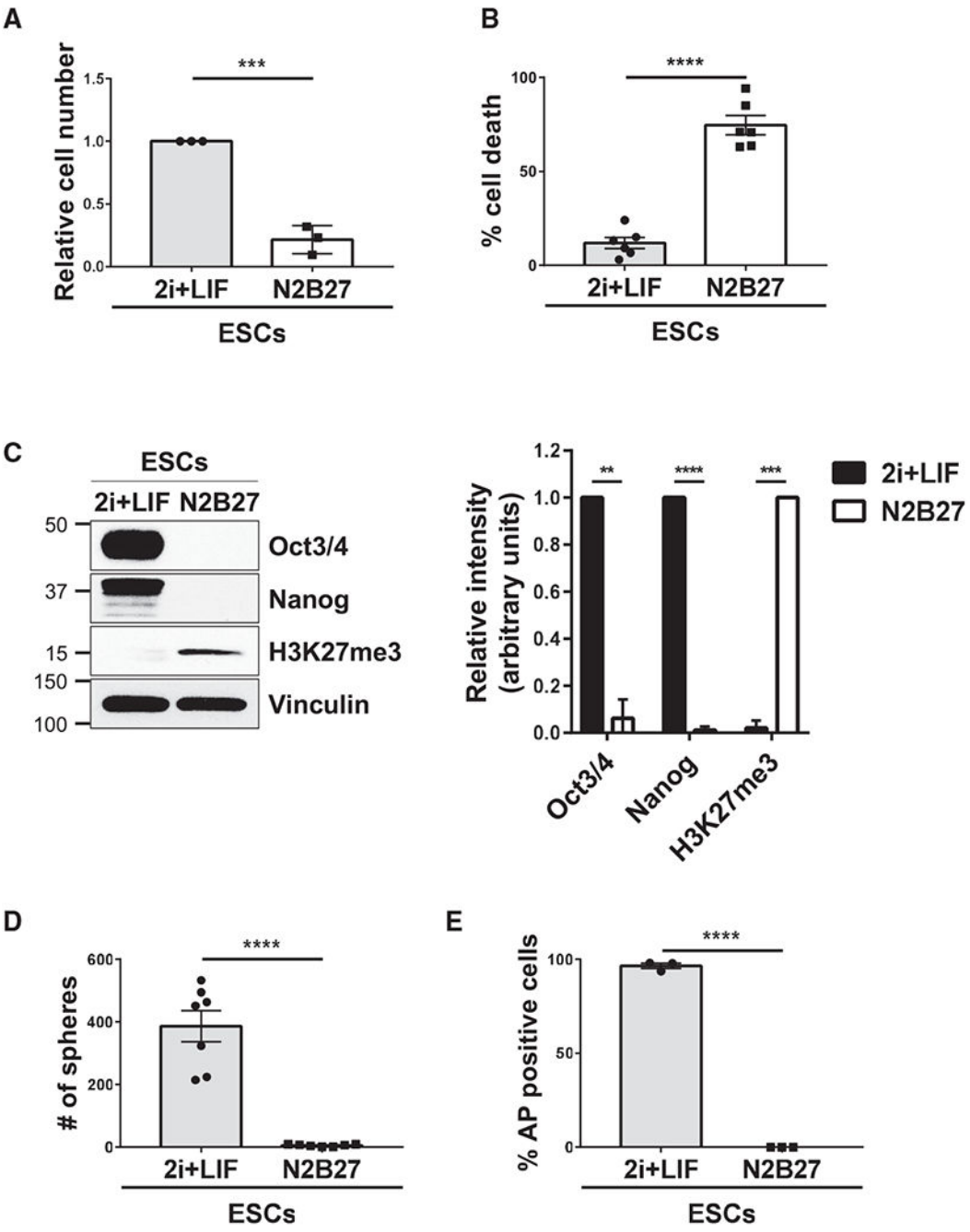

Figure 2. ESCs Lose Their Stem Cell Phenotypes When Cultured in N2B27 Medium

(A) Cell growth assays were performed on ESCs maintained in 2i+LIF or N2B27 medium.*

(B) Cell death assays were performed on ESCs maintained in 2i+LIF or N2B27 medium.*

(C) ESCs cultured in 2i+LIF or N2B27 medium were immunoblotted for Oct3/4, Nanog, the trimethylation of lysine 27 in histone H3 (H3K27me3), and vinculin as the loading control.*

(D) Sphere formation assays were performed on ESCs maintained in 2i+LIF or N2B27 medium. See corresponding images in Figure S2B.*

(E) AP activity assays were performed on ESCs maintained in 2i+LIF or N2B27 medium. See corresponding images in Figure S2C.*

*The data shown in (A)–(E) are presented as mean ± SD. All experiments were performed at least three independent times, and statistical significance was determined using Student's t test; ****$p < 0.0001$; ***$p < 0.001$; and **$p < 0.01$. See also Figure S2.

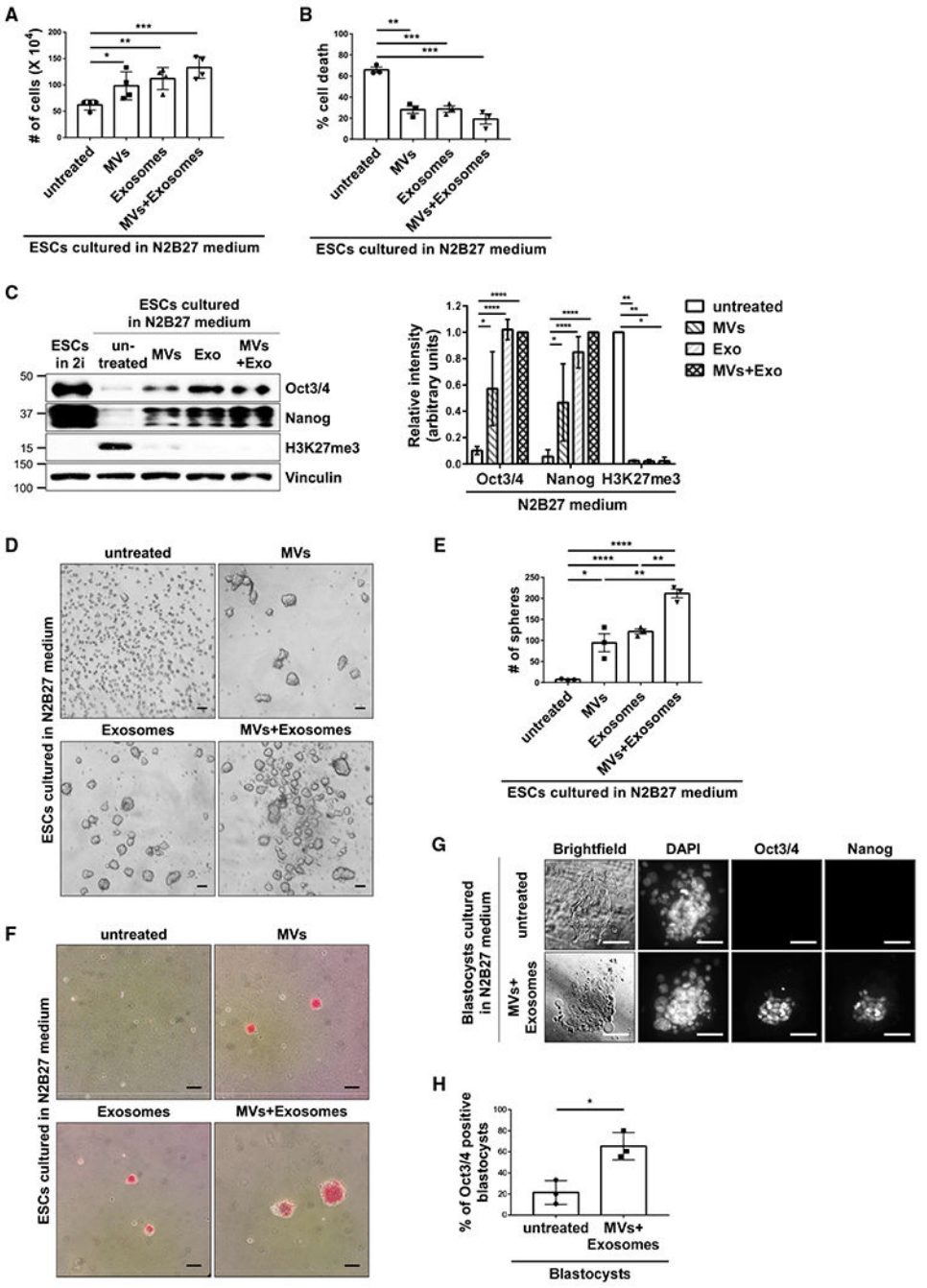

Figure 3. EVs from ESCs Promote Stem-Cell-Related Phenotypes

(A) Cell growth assays were performed on ESCs cultured in N2B27 medium supplemented without (untreated) or with MVs and/or exosomes from ESCs.*

(B) Cell death assays were performed on ESCs cultured in N2B27 medium supplemented without (untreated) or with MVs and/or exosomes from ESCs.*

(C) ESCs cultured in 2i+LIF medium (lane 1) or N2B27 medium supplemented without (untreated) or with MVs and/or exosomes from ESCs (lanes 2–5) were immunoblotted for Oct3/4, Nanog, H3K27me3, and vinculin as the loading control.*

(D) Images of sphere formation assays performed on ESCs cultured in N2B27 medium supplemented without (untreated) or with MVs and/or exosomes from pluripotent ESCs. Scale bar, 100 μm.

(E) Quantification of the assays shown in (D).*

(F) Images of AP activity assays performed on ESCs cultured in N2B27 medium supplemented without (untreated) or with MVs and/or exosomes from ESCs. Cells positive for AP activity are red. Scale bar, 100 μm.

(G) Brightfield and fluorescent microscopy images of blastocysts isolated from pregnant mice cultured in N2B27 medium supplemented without (untreated) or with MVs and exosomes from ESCs. The blastocysts were stained for Oct3/4 and Nanog, and DAPI was used to label nuclei. Scale bar, 50 μm.

(H) Quantification of Oct3/4-positive blastocysts for each condition shown in (G). This assay was performed three separate times, with a minimum of 13 blastocysts being evaluated per condition in each assay, before the results were averaged and plotted.*

*The data shown in (A)–(C), (E), and (H) are presented as mean ± SD. All experiments were performed at least three independent times, and statistical significance was determined using Student's t test; ****$p < 0.0001$; ***$p < 0.001$; **$p < 0.01$; and *$p < 0.05$. See also Figure S3.

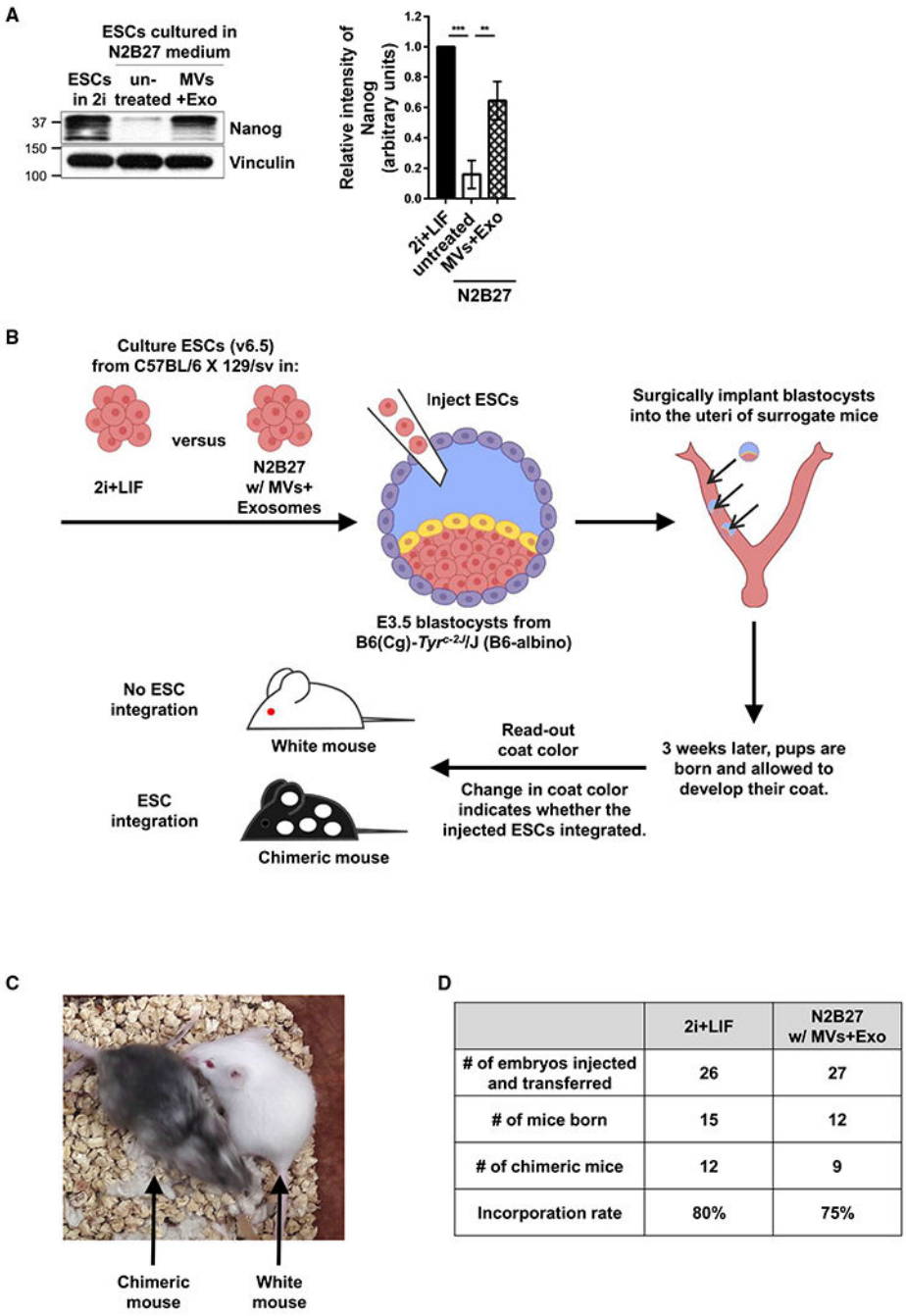

	2i+LIF	N2B27 w/ MVs+Exo
# of embryos injected and transferred	26	27
# of mice born	15	12
# of chimeric mice	12	9
Incorporation rate	80%	75%

Figure 4. EVs from ESCs Help Maintain the Ability of ESCs to Incorporate into a Developing Embryo and Generate a Chimeric Animal

(A) v6.5 mouse ESCs cultured in 2i+LIF medium, or N2B27 medium supplemented without (untreated) or with MVs and exosomes from ESCs for 30 h were immunoblotted for Nanog and vinculin as the loading control.*

(B) Diagram depicting the experiment used to show whether the ESCs treated with EVs were capable of generating chimeric mice. v6.5 mouse ESCs grown in 2i+LIF medium or N2B27 medium supplemented with MVs and exosomes from ESCs were injected into embryonic day 3.5 (E3.5) blastocysts and surgically implanted into the uteri of surrogate

mice. The ability of the cells to successfully incorporate into the embryos was evaluated by a change in coat color.

(C) Image showing an example of a chimeric mouse (i.e., ESCs successfully integrated) and a mouse with a white coat (i.e., ESCs failed to integrate).

(D) Table showing the number of embryos injected and transferred, the number of mice born, the number of chimeric mice born, and the integration rates of ESCs grown in 2i+LIF versus N2B27 medium supplemented with MVs and exosomes isolated from pluripotent ESCs.

*The data shown in (A) are presented as mean ± SD. The experiment was performed at least three independent times, and statistical significance was determined using Student's t test; ***$p < 0.001$ and **$p < 0.01$.

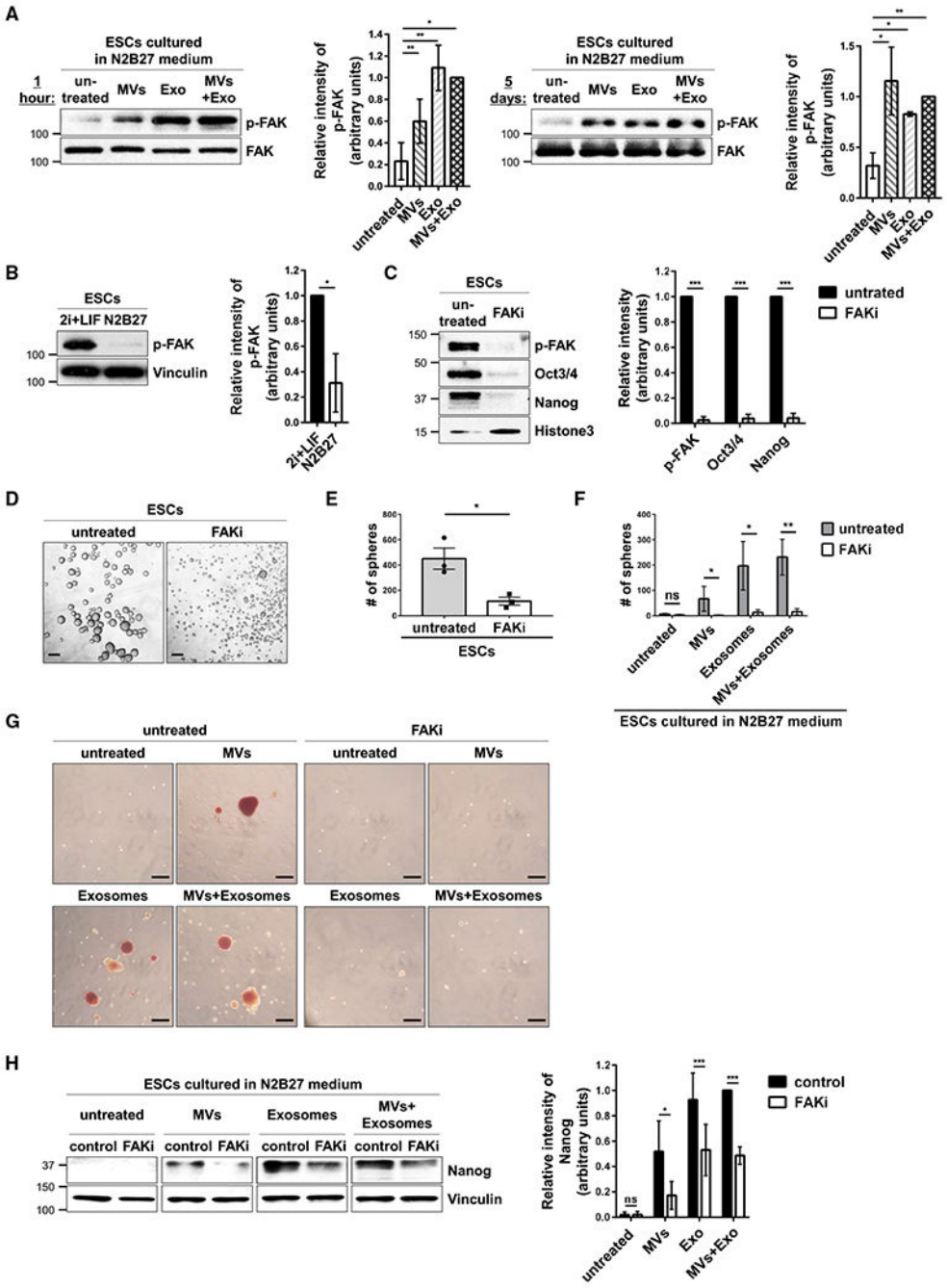

Figure 5. EVs from ESCs Help Maintain Stemness by Activating FAK in Recipient Cells

(A) ESCs cultured in N2B27 medium supplemented without (untreated) or with MVs and/or exosomes from ESCs for 1 h (left) and 5 days (right) were immunoblotted for phosphorylated FAK (p-FAK) and total FAK.*

(B) ESCs cultured in 2i+LIF or N2B27 medium were immunoblotted for phosphorylated FAK (p-FAK) and vinculin.*

(C) ESCs cultured in 2i+LIF medium supplemented without (untreated) or with 7.5 μM FAK inhibitor III (FAKi) were immunoblotted for phosphorylated FAK (p-FAK), Oct3/4, Nanog, and histone 3 as the loading control.*

(D) Images of sphere formation assays performed on ESCs maintained in 2i+LIF medium supplemented without (untreated) or with 7.5 μM FAK inhibitor III (FAKi). Scale bar, 100 μm.

(E) Quantification of the assays shown in (D).*

(F) Quantification of sphere formation assays performed on ESCs cultured in N2B27 medium supplemented with MVs and/or exosomes produced by ESCs and treated without (untreated, shaded bars) or with 7.5 μM FAK inhibitor III (FAKi, clear bars).*

(G) Images of AP activity assays performed on ESCs cultured in N2B27 medium supplemented with MVs and/or exosomes from ESCs and treated without (untreated) or with 7.5 μM FAK inhibitor III (FAKi). Scale bar, 100 μm.

(H) ESCs cultured in N2B27 medium supplemented with MVs and/or exosomes from ESCs and treated without (control) or with 7.5 μM FAK inhibitor III (FAKi) were immunoblotted for Nanog and vinculin as the loading control.*

*The data shown in (A)–(C), (E), (F), and (H) are presented as mean ± SD. All experiments were performed at least three independent times, and statistical significance was determined using Student's t test; ***$p < 0.001$; **$p < 0.01$; *$p < 0.05$; and ns, not significant. See Figures S4–S6.

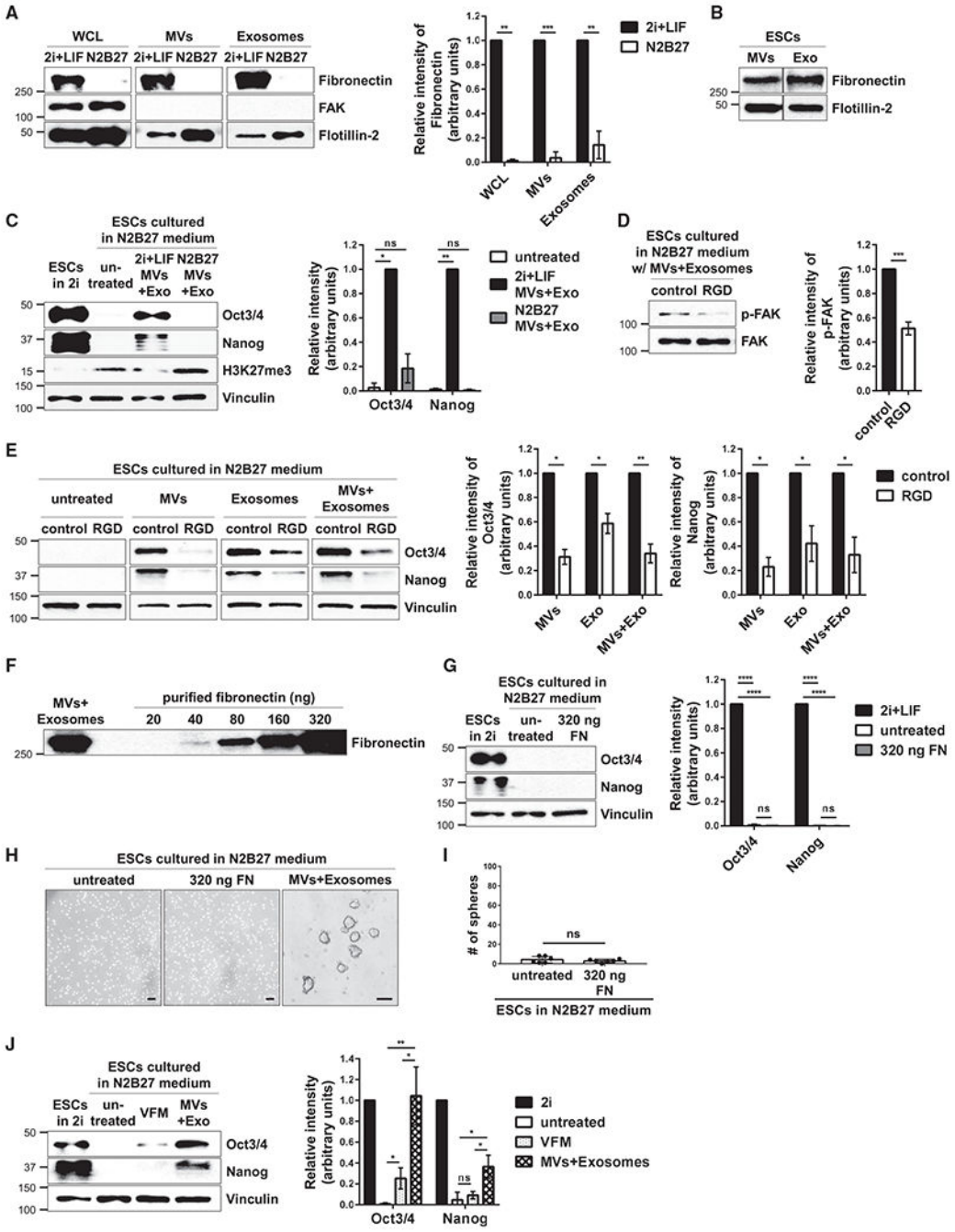

Figure 6. Fibronectin Associated with EVs from ESCs Is Important for Promoting Stemness

(A) ESCs cultured in 2i+LIF or N2B27 medium, as well as the MVs and exosomes isolated from these cells, were immunoblotted for fibronectin, the cytosolic protein FAK, and the general EV marker Flotillin-2.*

(B) MVs and exosome (Exo) preparations isolated from ESCs using the procedure described in Figure S1G were further resolved by sucrose density gradient ultracentrifugation. The intermediate-density fraction collected from each preparation was lysed and immunoblotted for fibronectin and the general EV marker Flotillin-2.

(C) ESCs maintained in N2B27 medium supplemented without (untreated) or with MVs and exosomes isolated from ESCs cultured in either 2i+LIF medium (2i+LIF MVs+Exo) or N2B27 medium (N2B27 MVs+Exo) were immunoblotted for Oct3/4, Nanog, H3K27me3, and vinculin as the loading control. ESCs grown in 2i+LIF medium were used as the positive control (first lane).

(D) ESCs cultured in N2B27 medium supplemented with MVs and exosomes from pluripotent ESCs and treated without (control) or with 25 μg/mL of the RGD peptide were immunoblotted for phosphorylated FAK (p-FAK) and total FAK.*

(E) ESCs cultured in N2B27 medium supplemented with MVs and/or exosomes from pluripotent ESCs and treated without (control) or with 25 μg/mL of the RGD peptide were immunoblotted for Oct3/4, Nanog, and vinculin as the loading control.*

(F) The amount of MVs and exosomes from ESCs that was used to promote stemness and the increasing amounts of purified fibronectin that were immunoblotted for fibronectin.

(G) ESCs cultured in N2B27 medium supplemented without (untreated) or with 320 ng of purified fibronectin (FN) were immunoblotted for Oct3/4, Nanog, and vinculin as the loading control. ESCs grown in 2i+LIF medium were used as the positive control (first lane).*

(H) Images of sphere formation assays performed on ESCs cultured in N2B27 medium supplemented without (untreated) or with 320 ng of purified fibronectin (FN) or MVs and exosomes from pluripotent ESCs. Scale bar, 100 μm.

(I) Quantification of the assays shown in (H).*

(J) ESCs cultured in N2B27 medium supplemented without (untreated) or with vesicle-free medium (VFM), or MVs and exosomes from ESCs (MVs+Exo), were immunoblotted for Oct3/4, Nanog, and vinculin as the loading control. ESCs grown in 2i+LIF medium were used as the positive control (first lane).*

*The data shown in (A), (C)–(E), (G), (I), and (J) are presented as mean ± SD. All experiments were performed at least three independent times, and statistical significance was determined using Student’s t test; ****$p < 0.0001$; ***$p < 0.001$; **$p < 0.01$; *$p < 0.05$; and ns, not significant. See also Figures S6 and S7.

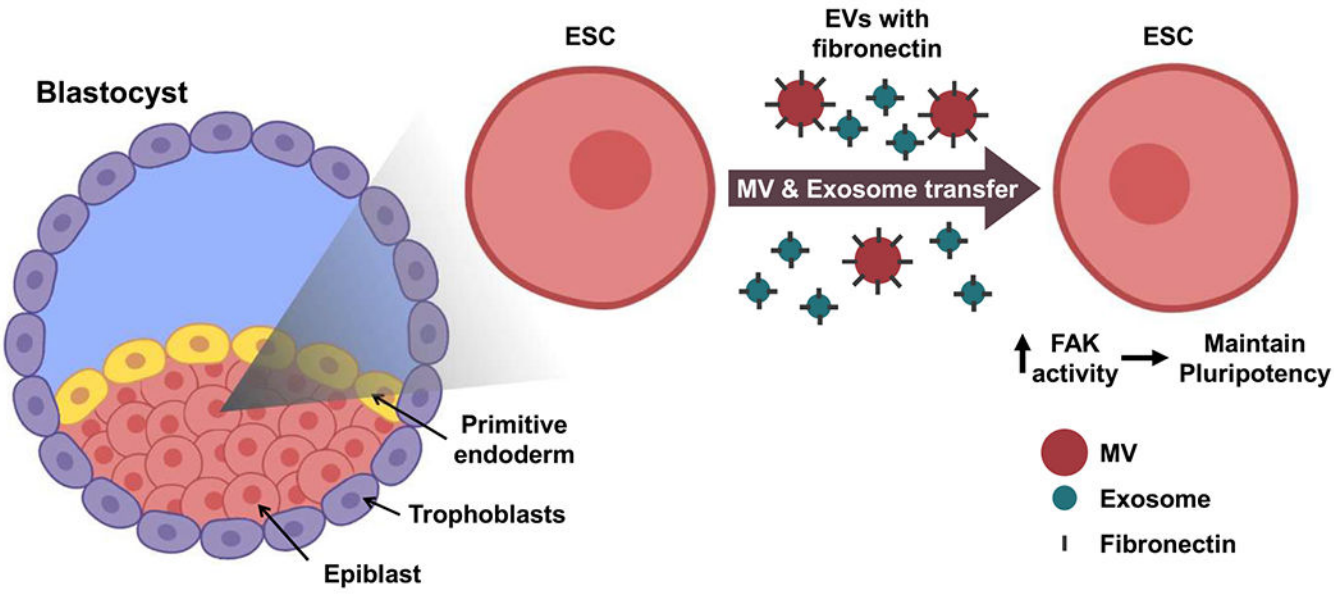

Figure 7. Diagram Depicting How EVs Are Used by Pluripotent Cells to Promote Stemness

Left: in the blastocyst-stage embryo, the ICM consists of the epiblast and the primitive endoderm and is surrounded by a layer of trophoblasts. The epiblast is where the pluripotent stem cells reside. Right: ESCs are considered to be the *in vitro* equivalents of epiblast cells, and they generate MVs and exosomes that have fibronectin associated with their surfaces. The transfer of ESC-derived EVs to other ESCs activates FAK and promotes pluripotency.

KEY RESOURCES TABLE

REAGENT or RESOURCE	SOURCE	IDENTIFIER
Antibodies		
CD9 antibody	Abcam	Cat# ab92726; RRID: AB_10561589
c-Myc antibody	Cell Signaling Technology	Cat# 5605; RRID: AB_1903938
FAK antibody	Cell Signaling Technology	Cat# 3285; RRID: AB_2269034
Fibronectin antibody	Sigma-Aldrich	Cat# F3648; RRID: AB_476976
FlotiNin-2 antibody	Cell Signaling Technology	Cat# 3436; RRID: AB_2106572
Klf4 antibody	Cell Signaling Technology	Cat# 4038; RRID: AB_2265207
Nanog antibody	Abcam	Cat# ab80892; RRID: AB_2150114
Oct3/4 antibody	Santa Cruz Biotechnology	Cat# sc-5279; RRID: AB_628051
Phospho-FAK (Tyr397) antibody	Cell Signaling Technology	Cat# 3283; RRID: AB_2173659
Sox2 antibody	Cell Signaling Technology	Cat# 4900; RRID: AB_10560516
Tri-Methyl-Histone H3 (Lys27) antibody	Cell Signaling Technology	Cat# 9733; RRID: AB_2616029
Vinculin antibody	Cell Signaling Technology	Cat# 13901; RRID: AB_2728768
Rabbit IgG-HRP conjugate antibody	Cell Signaling Technology	Cat# 7074; RRID: AB_2099233
Mouse IgG-HRP conjugate antibody	Cell Signaling Technology	Cat# 7076; RRID: AB_330924
Mouse IgG-Alexa 488 conjugate antibody	Thermo Fisher Scientific	Cat# A-11029; RRID: AB_2534088
Rabbit IgG-Alexa 568 conjugate antibody	Thermo Fisher Scientific	Cat# A-11036; RRID: AB_10563566
Chemicals, Peptides, and Recombinant Proteins		
Aprotinin	Sigma-Aldrich	Cat# 10236624001
B-27 supplement	Thermo Fisher Scientific	Cat# 17504044
Bio-Rad protein assay	Bio-Rad	Cat# 5000006
CHIR99021	Selleckchem	Cat# S1263
DAPI	Sigma-Aldrich	Cat# D9542
Dimethylsulfoxide (DMSO)	Sigma-Aldrich	Cat# D8418
Dithiothreitol (DTT)	Sigma-Aldrich	Cat# 10197777001
DMEM	Gibco	Cat# 11965-092
DMEM/F12	Gibco	Cat# 12634-010
Western Lightning Plus-ECL	Perkin-Elmer	Part# NEL105001EA
FAK inhibitor III	Sigma-Aldrich	Cat# 5040450001
Y15	Sigma-Aldrich	Cat# SML0837
Fetal bovine serum	Gibco	Cat# 10437028
Fibronectin (Bovine plasma)	Millipore	Cat# 341631
FM1-43FX	Thermo Fisher Scientific	Cat# F35355
Gly-Arg-Gly-Asp-Ser-Pro (GRGDSP)	Sigma-Aldrich	Cat# SCP0157
KSOM medium	Sigma-Aldrich	Cat# MR-101-D
L-Ascorbic acid	Millipore	Cat# 1831
Leukemia inhibitory factor (mouse)	Millipore	Cat# ESG1107

REAGENT or RESOURCE	SOURCE	IDENTIFIER
Leupeptin	Sigma-Aldrich	Cat# L9783
L-Glutamine	Sigma-Aldrich	Cat# G8540
M2 medium	Sigma-Aldrich	Cat# MR-015-D
Monothioglycerol	Sigma-Aldrich	Cat# M6145
N-2 supplement	Thermo Fisher Scientific	Cat# 17502048
Neurobasal medium	Gibco	Cat# 21103049
Phosphate buffered saline tablets	VWR	Cat# VWRVE404
PD03259010	Selleckchem	Cat# S1036
Pen-Strep	Gibco	Cat# 15140122
RNase A	Thermo Fisher Scientific	Cat# EN0531
StemPro accutase	Thermo Fisher Scientific	Cat# A1110501
Trypan Blue solution 0.4 %	Gibco	Cat# 15250061
Trypsin-EDTA (0.05 %)	Gibco	Cat# 25300054
Critical Commercial Assays		
VECTOR Red Alkaline phosphatase substrate kit	VECTOR laboratories	Cat# SK-5100
RNeasy mini kit	QIAGEN	Cat# 74104
Superscript III Reverse transcriptase	Invitrogen	Cat# 18080044
Deposited Data		
Unprocessed blots	This paper	https://doi.org/10.17632/mt4gm74tbw.1
Experimental Models: Cell Lines		
Mouse: E14tg2a.4	ATCC	Cat# CRL-1821
Mouse: Mouse Embryonic Fibroblasts	Cornell's Stem Cell and Transgenic Core Facility	N/A
Mouse: NIH3T3	ATCC	Cat# CRL-1658
Mouse: v6.5	Provided by Cornell's Stem Cell and Transgenic Core Facility, Cornell University	N/A
Oligonucleotides		
Primer: Oct3/4 Forward: GTTGGAGAAGGTGGAACCAA	This paper	N/A
Primer: Oct3/4 Reverse: CCAGTCACACCCAACCTCTT	This paper	N/A
Primer: Nanog Forward: CATGTTTAAGGTCGGGCTGT	This paper	N/A
Primer: Nanog Reverse: AAAGAGTGCGTGGAGGAAGA	This paper	N/A
Primer: Sox2 Forward: AGGGCTGGGAGAAAGAAGAG	This paper	N/A
Primer: Sox2 Reverse: TTGCTGATCTCCGAGTTGTG	This paper	N/A
Primer: Klf4 Forward: CAGCTTCATCCTCGTCTTCC	This paper	N/A
Primer: Klf4 Reverse: CGCCTCTTGCTTAATCTTGG	This paper	N/A
Primer: c-Myc Forward: ATGCATTTTGAAGCGGGGTT	This paper	N/A
Primer: c-Myc Reverse: CAACGAATCGGTCACATCCC	This paper	N/A
Primer: Lin28 Forward: AGGAGAAGCTGAGGTGTCCA	This paper	N/A

REAGENT or RESOURCE	SOURCE	IDENTIFIER
Primer: Lin28 Reverse: ACAAGTGTTGGGCCTATTGC	This paper	N/A
Primer: GAPDH Forward: CTCAGCTCCCCTGTTTCTTG	This paper	N/A
Primer: GAPDH Reverse: CCTTCCACAATGCCAAAGTT	This paper	N/A
Primer: β-actin Forward: TGTTACCAACTGGGACGACA	This paper	N/A
Primer: β-actin Reverse: GACATGCAAGGAGTGCAAGA	This paper	N/A
Recombinant DNA		
pLV-neo-CD2-FAK	Shibue and Weinberg, 2009	Addgene Plasmid #37013
Software and Algorithms		
ImageJ	NIH	https://imagej-nih-gov.proxy.library.cornell.edu/ij/
IPLABs	BD Biosciences	N/A
Prism	Graphpad	https://www.graphpad.com
Other		
0.22 mm Steriflip filter	Millipore	Cat# SEM1M179M6
Amicon Ultra-15 centrifugal filter units – 100 Kda	Millipore	Cat# UFC910024
NanoDrop spectrophotometer	Thermo Fisher Scientific	Cat# 840-274200
NanoSight NS300	Malvern	N/A
Nunc Lab-Tek 8 well permanox chamber slide	Thermo Fisher Scientific	Cat# 177445
SW 41 Ti rotor	Beckman Coulter	N/A
Type 45 Ti rotor	Beckman Coulter	N/A
Ultra low attachment plate (6 well)	Corning	Cat# 3471